

# Fairness Increases Adversarial Vulnerability

Cuong Tran  
Syracuse University  
cutran@syr.edu

Keyu Zhu  
Georgia Tech  
kzhu67@gatech.edu

Ferdinando Fioretto  
Syracuse University  
ffiorett@syr.edu

Pascal Van Hentenryck  
Georgia Tech  
pvh@isye.gatech.edu

## Abstract

*The remarkable performance of deep learning models and their applications in consequential domains (e.g., facial recognition) introduces important challenges at the intersection of equity and security. Fairness and robustness are two desired notions often required in learning models. Fairness ensures that models do not disproportionately harm (or benefit) some groups over others, while robustness measures the models' resilience against small input perturbations.*

*This paper shows the existence of a dichotomy between fairness and robustness, and analyzes when achieving fairness decreases the model robustness to adversarial samples. The reported analysis sheds light on the factors causing such contrasting behavior, suggesting that distance to the decision boundary across groups as a key explainer for this behavior. Extensive experiments on non-linear models and different architectures validate the theoretical findings in multiple vision domains. Finally, the paper proposes a simple, yet effective, solution to construct models achieving good trade-offs between fairness and robustness.*

## 1. Introduction

Data-driven learning systems have become instrumental for decision-making in a variety of consequential contexts. They include assistance in legal decisions [16], lending [33], hiring [30], performing personalized ads targeting [6], and providing personalized recommendations [4]. As a result, fairness has become a crucial requirement for their successful use and adoption. Various notions of fairness drawing from legal and philosophical doctrine have been proposed to ensure that the models errors do not disproportionately affect the decisions of some groups over others [25]. In general, fair models attempt at constraining their hypothesis space so that the errors of the reported outcomes are distributed uniformly across different protected groups.

When these fairness constraints are enforced in learning systems, a commonly observed behavior is an overall degradation of the model accuracy. Thus, a growing body of research has been focusing on striking the right balance

between fairness and accuracy [29]. This paper shows that fairness may have another important consequence on the deployed models: *a reduction of the model robustness*. This aspect is important as the vulnerability of deep learning models to adversarial examples hinders their application in many security-sensitive domains. However, these behaviors are currently not fully understood and have not received the attention they deserve given the significant equity and security consequences they have on the final decisions.

This paper addresses this important gap and shows that enforcing fairness may negatively affect the robustness of a model. In particular, the paper makes the following contributions: (1) it analyzes when and why fairness and robustness may be misaligned in their objectives, (2) it provides an analysis on the relationship between fair, robust, and "natural" (e.g., non-fair non-robust) models, and (3) it identifies *the distance to the decision boundary* as a key aspect linking fairness and robustness. Moreover, (4) the paper shows how the distance to the decision boundary can explain the increase of adversarial vulnerability of fair models, providing extensive experiments and validation over a variety of vision tasks and architectures, and verifying the presence of the fairness/robustness dichotomy for multiple techniques aimed at achieving fairness and measuring robustness. Finally, (5) building from the reported theoretical observations, the paper also proposes a simple, yet effective, strategy to find a good tradeoff between accuracy, fairness, and robustness.

To the best of the authors' knowledge, this is the first work showing that enforcing fairness may negatively affect robustness. The results show that, without careful considerations, inducing a desired equity property on a learning task may create significant security challenges. These results should not be read as an endorsement to avoid constructing fairer or safer models; rather it should be understood as a call for additional research at the intersection of fairness and robustness to achieve appropriate tradeoffs.

## 2. Related work

**Fairness.** Models that learn from rich datasets have been shown to carry over bias which may induce to disproportionately harm some groups of individuals (often identified

by their race or gender) over others [3, 19, 39]. These observations have resulted in a whole new research area that has focused on defining, analyzing, and mitigating unfairness [8, 45]. The source of the observed unfairness has been often attributed to data properties [5, 25, 34] or different aspects of the model’s properties [35, 38]. For example, imbalance in groups’ size is commonly argued to create disparities in the task’s performance [25]. It has also been shown that constraining the model’s hypothesis space to satisfy privacy [2], sparsity [14, 15], or robustness [26, 44] can result in disparate outcomes.

**Robustness.** Deep Neural Networks (DNNs) have been shown to be susceptible to carefully crafted adversarial perturbations which—imperceptible to a human—result in a misclassification by the model [36]. The literature on the topic attributes the reason for such behavior to arise to three key factors: data properties, network architecture, and model training. For example, [11, 31] observed that the input dimension plays a decisive role in the robustness of a model, with larger inputs yielding more brittle models. Likewise, the ability of some architectures to capture high frequency spectrum of image data (that are almost imperceptible to a human) relates to the success of devising adversarial examples in the underlying models [41]. With respect to the network architecture, it has been observed that some network architectures may render the underlying model more or less brittle to adversarial inputs. For example, batch-normalization is cited to the models’ robustness [9], some shift-invariant architectures, such as CNNs, are more vulnerable to adversarial inputs compared to other architectures, e.g., fully connected networks. Finally, Yao et al. [46] empirically observed that model trained with large batch-sizes can be more easily fooled by adversarial inputs when compared to models trained with smaller batch sizes.

**Robustness and fairness.** This work lies in the intersection of fairness and robustness. Within this context, recently Xu et al [44] has shown that adversarially robust models exhibit remarkable disparity of natural accuracy and robust accuracy metrics among different classes, compared to those exhibited by their standard counterpart. Khani and Liang [17] analyze why noise in features can cause disparity in error rates when learning a regression.

We believe this is the first work to show that enforcing fairness may negatively affect a model’s robustness and hope that this result will lead to further strengthening the interconnection of these two important machine learning areas.

### 3. Problem Settings

The paper considers a typical multi-class classification problem, whose input is a dataset  $D$  consisting of  $n$  data points  $(X_i, A_i, Y_i)$ , each of which drawn i.i.d. from an unknown distribution  $\Pi$  and where  $X_i \in \mathcal{X}$  is a feature vector,  $A_i \in \mathcal{A}$  is a protected attribute, and  $Y_i \in \mathcal{Y} = [C]$  is a label,

with  $C$  being the number of possible class labels. For example, consider the case of a classifier to predict the age range of an individual. The features  $X_i$  may describe the pixels associated with the individual headshot and their demographics, the protected attribute  $A_i$  may describe the individual gender or ethnicity, and  $Y_i$  represents the age range. The goal is to learn a classifier  $f_\theta : \mathcal{X} \rightarrow \mathcal{Y}$ , where  $\theta$  is a vector of real-valued parameters. The model quality is assessed in terms of a non-negative loss function  $\ell : \mathcal{Y} \times \mathcal{Y} \rightarrow \mathbb{R}_+$ , and the training aims at minimizing the empirical risk function:

$$\hat{\theta} = \underset{\theta}{\operatorname{argmin}} \mathcal{L}_\theta(D) \left( = \frac{1}{n} \sum_{i=1}^n \ell(f_\theta(X_i), Y_i) \right) \quad (1)$$

For a group  $a \in \mathcal{A}$ , notation  $D_a$  is used to denote the subset of  $D$  containing exclusively samples  $i$  with  $A_i = a$ . Importantly, the paper assumes that the attribute  $A$  is not part of the model input during inference. The paper focuses on learning classifiers that satisfy group fairness (to be defined shortly) and on analyzing the robustness impact of fairness.

## 4. Preliminaries

### 4.1. Fairness and fair learning

This paper considers a classifier  $f$  satisfying accuracy parity [49], a group fairness notion commonly adopted in machine learning requiring model misclassification rates to be conditionally independent of the protected attribute. That is,  $\forall (X, Y, A) \sim \Pi$  and  $\forall a \in \mathcal{A}$ ,

$$|\Pr(f_\theta(X) \neq Y \mid A = a) - \Pr(f_\theta(X) \neq Y)| \leq \alpha, \quad (2)$$

where  $\alpha$  denotes the allowed *fairness violation*. In practice, the above is expressed as a difference of empirical expectations of the group and population misclassification rates. That is,  $\forall a \in \mathcal{A}$ :

$$\left| \frac{1}{|D_a|} \sum_{(X, A, Y) \in D_a} \mathbb{1}\{f_\theta(X) \neq Y\} - \frac{1}{n} \sum_{(X, A, Y) \in D} \mathbb{1}\{f_\theta(X) \neq Y\} \right| \leq \alpha.$$

Several approaches have been proposed in the literature to encourage the satisfaction of accuracy parity. They can be summarized in methods that use penalty terms into the empirical risk loss function to capture the fairness violations, and those which minimize the maximum group loss. The core of the paper focuses on the first set of methods; the analysis for the second set is presented in Appendix B.

**Penalty-based methods.** In this category, the model loss function (Equation (1)) is augmented with penalty fairness constraint terms [1, 40] as follows:

$$\theta_f(\lambda) = \underset{\theta}{\operatorname{argmin}} \mathcal{L}_\theta(D) + \lambda \left( \sum_{a \in \mathcal{A}} |\mathcal{L}_\theta(D_a) - \mathcal{L}_\theta(D)| \right) \quad (3)$$

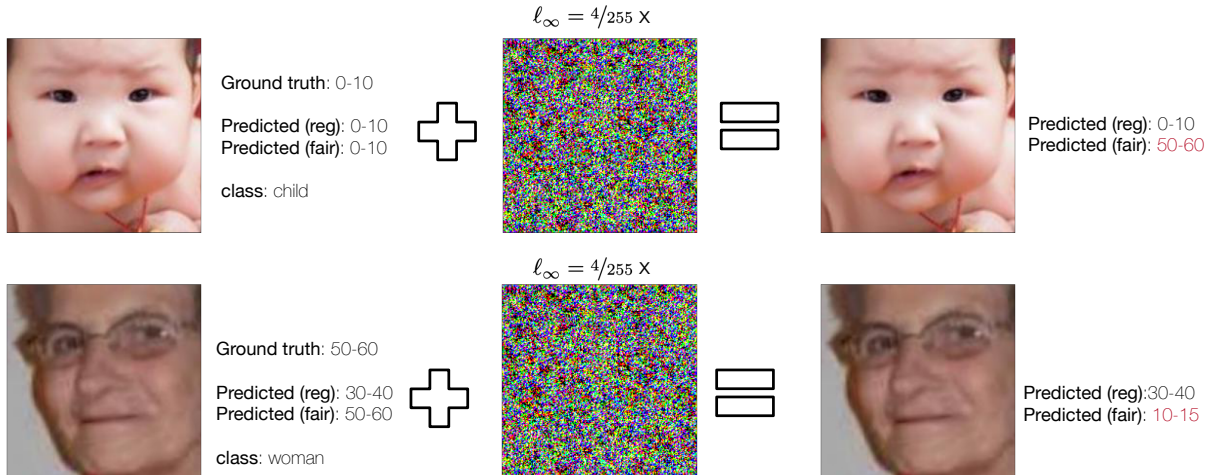


Figure 1. An example of robustness loss in the UTKFace dataset. A regular (reg) and a fair models are trained to predict age group from faces and exposed to adversarial examples generated under an RFGSM [37] attack. The predictions of the regular model do not change under adversarial examples (regardless of their original correctness), while the fair models decision change in the presence of adversarial noise.

where  $\mathcal{L}_\theta(D_a) = 1/|D_a| \sum_{(X,A,Y) \in D_a} \ell(f_\theta(X), Y)$  is the empirical risk loss associated with protected group  $a \in \mathcal{A}$ . In addition,  $\lambda > 0$  is the fairness penalty parameter that enforces a tradeoff between fairness and accuracy.

## 4.2. Robustness and Robust Learning

This paper analyzes the effect of enforcing fairness on adversarial robustness, a key property of trustworthy machine-learning systems. In this work, and following robust learning conventions, the robustness of a model  $f$  is measured in terms of the *robust error*:

$$\mathcal{L}_\theta^{\text{rob}}(\epsilon) = \Pr(\exists \tau, \|\tau\|_p \leq \epsilon, f_\theta(X + \tau) \neq Y), \quad (4)$$

which measures the sensitivity of the model errors to small input perturbations  $\|\tau\|_p \leq \epsilon$  in  $\ell_p$  norms, with  $p$  often considered in  $\{0, 1, 2, \infty\}$ . The robust error can be decomposed into two components [47]:

$$\mathcal{L}_\theta^{\text{rob}}(\epsilon) = \mathcal{L}_\theta^{\text{nat}} + \mathcal{L}_\theta^{\text{bdy}}(\epsilon), \quad (5)$$

where the first denotes the *natural error* and the second the *boundary error*. The natural error measures the standard model performance when exposed to *unperturbed* samples  $(X, A, Y)$ :

$$\mathcal{L}_\theta^{\text{nat}} = \Pr(f_\theta(X) \neq Y), \quad (6)$$

whose empirical version is defined in Equation (1) with a 0/1 loss function. The boundary error measures the probability that the model predictions change on *perturbed* samples  $(X + \|\tau\|_p, A, Y)$ :

$$\mathcal{L}_\theta^{\text{bdy}}(\epsilon) = \Pr(\exists \|\tau\|_p \leq \epsilon, f_\theta(X + \tau) \neq f_\theta(X), f_\theta(X) = Y). \quad (7)$$

The boundary error implicitly introduces a notion of *decision boundary* and a *distance between an input sample and this decision boundary*. For instance, in linear classifiers, the decision boundary is represented by an hyperplane. The distance of a sample  $X$  to the decision boundary for a classifier  $f_\theta$  can be formalized as

$$\Delta(X, f_\theta) = \max \epsilon \text{ s.t. } f_\theta(X + \tau) = f_\theta(X), \forall \|\tau\| \leq \epsilon.$$

Samples close to the decision boundary will be less tolerant to noise than those lying far from it. The analysis in this paper regarding the impact of fairness on robustness is based on this concept. In particular, the results show that imposing fairness constraints may reduce the distance to the decision boundary of the samples  $(X, A, Y) \sim \Pi$ .

## 5. Real-World Implications

Prior diving into the analysis, the paper provides an example showing how robustness errors can be exacerbated when a image classifier is trained to satisfy fairness. Deep neural networks have been used in many real-world applications, including image facial recognition and object detection. When perturbations (either due to noise or by malicious adversaries) are introduced in the model inputs, they may cause harmful effects as they lead the classifier to misclassify targeted inputs.

Figure 1 shows an example of inputs from the UTKFace dataset where a classifier is trained to minimize the regular empirical risk loss of equation (1) (top) or the fair empirical risk loss of equation (3) (bottom). Both inputs are perturbed with the same amount of  $\ell_\infty$  noise, but the fair network is much more brittle than its regular counterpart, inducing errors in the classifier outputs. It is important to note that this

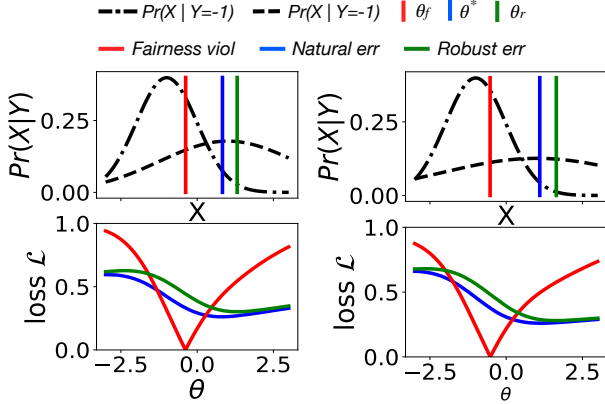


Figure 2. Illustration of optimal natural  $\theta^*$ , fair  $\theta_f$ , and robust  $\theta_r$  classifiers for  $K = 5$  (left) and  $K = 10$  (right) with  $\mu_- = -1$  and  $\mu_+ = 1$ .

paper uses datasets such as UTKFace (described in detail in Appendix C) only to demonstrate the effects of fairness to robustness. As noted in previous works, the very task of predicting gender, race, or other characteristics from a person face is flawed and raises deep ethical concerns [28].

## 6. Why Fairness Weakens Robustness?

This section presents the main results of the paper. It will show that fairness affects model robustness because the learned decision boundary is *pulled in opposite directions* by fair and robust models. To render the analysis tractable, the theoretical discussion focuses on linear classifiers, and more specifically on learning a mixture of Gaussians with a linear classifiers. In addition, Section 7 will show that a similar phenomenon occurs in large non-linear models. This section assumes that  $\mathcal{A} = \mathcal{Y}$ , i.e., the protected attribute is also the output of the classifier, again to simplify exposition. All proofs are given in Appendix A.

### Optimal Models for Mixtures of Gaussians

Consider a binary classification setting (i.e.,  $\mathcal{Y} = \{-1, 1\}$ ) with data drawn from a mixture of Gaussian distributions, so that  $\Pr(X | Y = -1) \propto \mathcal{N}(\mu_-, 1)$  and  $\Pr(X | Y = 1) \propto \mathcal{N}(\mu_+, K^2)$ , with  $\mu_- < \mu_+$  and different variances ( $K > 1$ ). The analysis can be easily extended to higher-dimensional cases, but these non-restrictive assumptions help simplifying and clarifying exposition. An illustration of this setting is reported in Figure 2 (top) where the data distributions are highlighted with black dashed curves.

The following analysis poses no restrictions on the relative subgroup sizes  $|D_1|$  and  $|D_{-1}|$  and focuses on the less-restrictive *balanced* data setting, in which data samples from different protected groups are equally likely.

The paper studies a family of parametric classifiers  $\{f_\theta\}_\theta$  with  $\theta \in [\mu_-, \mu_+] \subseteq \mathbb{R}$ , where  $f_\theta(X) = \mathbb{1}\{X > \theta\}$  denotes the classification output of the classifier. The optimal models with respect to the natural, fair, and robust losses can be specified as follows:

- **Optimal natural model** ( $f_{\theta^*}$ ). It is the Bayes classifier which minimizes the natural classification error as defined in Equation (1). In Figure 2 (top), this classifier is represented by vertical blue lines.
- **Optimal fair model** ( $f_{\theta_f}$ ). Intuitively, this classifier is  $\theta_f(\infty)$  as defined in Equation (3). Formally speaking, this classifier minimizes a lexicographic function whose first component is  $|\sum_{a \in \mathcal{A}} (\mathcal{L}_\theta(D_a) - \mathcal{L}_\theta(D))|$  and second component is  $\mathcal{L}_\theta(D)$ . In Figure 2 (top), this classifier is represented by vertical red lines.
- **Optimal robust model** ( $f_{\theta_r^{(\epsilon)}}$ ). This classifier minimizes the robust classification error in Equation (5), for a given  $\epsilon$ . In Figure 2 (top), it is depicted by vertical green lines.

### Relationships Between the Optimal Models

The next result characterizes the positional relationship among the three optimal models mentioned above, which can be observed in Figure 2.

**Theorem 6.1.** For any  $\epsilon \in [0, \frac{\mu_+ - \mu_-}{2}]$  and  $K \in (1, B_K]$ , where  $B_K = \min \left\{ \exp \left( \frac{(\mu_+ - \mu_- - 2\epsilon)^2}{2} \right), \frac{\mu_+ - \mu_-}{\epsilon} - 1 \right\}$ ,

$$\mu_- + \epsilon \leq \theta_f \leq \hat{\theta} \leq \theta_r^{(\epsilon)} \leq \mu_+ - \epsilon. \quad (8)$$

Besides,  $\theta_r^{(\epsilon)}$  is an increasing function of  $\epsilon$  over  $\left[0, \frac{\mu_+ - \mu_-}{2}\right]$ .

The result follows from the observation that the optimal natural model  $f_{\theta^*}$  can be expressed as

$$\hat{\theta} = \mu_- - \frac{\mu_+ - \mu_-}{K^2 - 1} + \frac{K}{K^2 - 1} \sqrt{2(K^2 - 1) \ln(K) + (\mu_+ - \mu_-)^2};$$

the fair classifier  $f_{\theta_f}$  as:

$$\theta_f = \mu_- + \frac{\mu_+ - \mu_-}{K + 1}$$

and the robust classifier  $f_{\theta_r^{(\epsilon)}}$  as

$$\theta_r^{(\epsilon)} = \mu_- - \frac{\mu_+ - \mu_- - (K^2 + 1)\epsilon}{K^2 - 1} + \frac{K}{K^2 - 1} \sqrt{2(K^2 - 1) \ln(K) + (\mu_+ - \mu_- - 2\epsilon)^2}.$$

From the result above, it follows that **(1)** the fair classifier achieves the largest robust error while the robust classifier



results in the least error, and (2) the fair classifier achieves the largest boundary error while the robust classifier results in the smallest boundary error, as expressed by the following Corollaries.

**Corollary 6.2.** For any  $\epsilon \in \left[0, \frac{\mu_+ - \mu_-}{2}\right]$  and  $K \in (1, B_K]$ ,

$$\mathcal{L}_{\theta_f}^{\text{rob}}(\epsilon) \geq \mathcal{L}_{\theta^*}^{\text{rob}}(\epsilon) \geq \mathcal{L}_{\theta_f^{(\epsilon)}}^{\text{rob}}(\epsilon).$$

**Corollary 6.3.** For any  $\epsilon \in \left[0, \frac{\mu_+ - \mu_-}{4}\right]$  and  $K \in (1, \bar{B}_K]$ ,

$$\mathcal{L}_{\theta_f}^{\text{bdy}}(\epsilon) \geq \mathcal{L}_{\theta^*}^{\text{bdy}}(\epsilon) \geq \mathcal{L}_{\theta_f^{(\epsilon)}}^{\text{bdy}}(\epsilon),$$

where  $\bar{B}_K = \min \left\{ \exp \left( \frac{(\mu_+ - \mu_- - 2\epsilon)^2}{2} \right), \phi^{-1} \left( \frac{\mu_+ - \mu_-}{\epsilon} - 2 \right) \right\}$  and  $\phi^{-1}$  is the inverse function associated with  $\phi : [1, +\infty) \mapsto [2, +\infty)$  such that  $\phi(x) = x + 1/x$ .

These results highlight the impossibility of achieving fairness and robustness simultaneously in this classification task. Fairness and robustness are pulling the classifier in opposite directions.

### The Role of the Decision Boundary

Building on the previous results, this section provides the key theoretical intuitions to explain why fairness increases adversarial vulnerability. It identifies the average distance to the decision boundary as the central aspect linking fairness and robustness, which is formalized in Theorem 6.4.

**Theorem 6.4.** For any  $\epsilon \in \left[0, \frac{\mu_+ - \mu_-}{2}\right]$  and  $K \in (1, B_K]$ ,

$$\mathbb{E} \left[ \Delta \left( X, f_{\theta_f^{(\epsilon)}} \right) \right] \geq \mathbb{E} \left[ \Delta \left( X, f_{\theta^*} \right) \right] \geq \mathbb{E} \left[ \Delta \left( X, f_{\theta_r} \right) \right].$$

In addition, the fair model minimizes the average distance to its decision boundary over all valid classifiers, i.e.,

$$\theta_f = \operatorname{argmin}_{\theta \in [\mu_-, \mu_+]} \mathbb{E} \left[ \Delta \left( X, f_{\theta} \right) \right].$$

This result indicates that, among the three considered optimal models, the fair model has the smallest average distance to the decision boundary. while the robust model has the largest distance. The result above is exemplified in Figure 2. The bottom plots show the losses associated with the optimal natural, fair, and robust models for two choices of  $K$  (left and right) while the top plots show the optimal decision boundaries associated with each of the three models – notice that they correspond to the minima of their relative losses.

Observe how class  $Y = 1$  has a higher classification error than class  $Y = -1$  under the natural (and thus unfair) classifier  $f_{\theta^*}$ . This is intuitive since the conditional distribution  $\Pr(X | Y = 1)$  has much higher variance than

$\Pr(X | Y = -1)$ . Hence, to balance the classification errors, the fair classifier pushes the decision boundary towards the mean of class  $Y = -1$ . This increases the error of class  $Y = -1$  while decreasing the error of class  $Y = 1$ . In contrast, the robust classifier pushes the decision boundary far away from the dense input region, i.e., the mean of the data associated with class  $Y = -1$ .

There are a few points worth emphasizing. First, *robustness and fairness pull the decision boundary into two opposite directions*. Second, the fair model  $f_{\theta_f}$  results in predictions with higher robust errors, when compared to the optimal natural model  $f_{\theta^*}$ , and it also increases adversarial vulnerability as the variance  $K$  increases. The variance  $K$  regulates the difference in the standard deviation of the underlying distributions associated with the protected groups and thus controls the overall distance to the decision boundary. *In summary, fairness can reduce the average distance of the training samples to the decision boundary which, in turn, makes the model less tolerant to adversarial noise.*

This section concludes with another important result. The previous relationships continue to hold even when the optimality conditions of the fair classifier are relaxed, i.e., when  $\lambda$  is taking values different from  $\infty$ . Moreover, the fairness constraints always reduce the distance to the decision boundary among protected groups and this reduction is proportional to the strength of the fairness constraints (or the tightness of the required fairness bound  $\alpha$ ).

**Theorem 6.5.** Consider the fair classifier  $f_{\theta_f(\lambda)}$  that optimizes Equation (3). It follows that, for any  $\lambda \in \left(\frac{K-1}{K+1}, +\infty\right)$ ,

$$\theta_f(\lambda) = \theta_f$$

while for any  $\lambda \in \left[0, \frac{K-1}{K+1}\right]$ ,  $\theta_f(\lambda) = \mu_- - \frac{\mu_+ - \mu_-}{K^2 - 1} + \frac{K}{K^2 - 1} \sqrt{2(K^2 - 1) \ln \left( \frac{1-\lambda}{1+\lambda} \cdot K \right) + (\mu_+ - \mu_-)^2}$ . Moreover, the parameter  $\theta$  associated with the fair classifier and the average distance to its decision boundary  $\mathbb{E} \left[ \Delta \left( X, f_{\theta_f(\lambda)} \right) \right]$  are both decreasing as  $\lambda$  increases.

Informally speaking, Theorem 6.5 states that applying fairness constraint with large enough penalty  $\lambda$  will push the decision boundary towards the negative class (group with smallest variance). As a result, the average distance to the decision boundary of all samples will be reduced.

While the analysis above applies to the linear setting considered in this section, the results were empirically validated on large non-linear models. For example, Figure 3 compares the performance of a penalty based fair CNN model (bottom plots) with  $\lambda = 1.0$  against a natural (non-fair) CNN classifier (top plots). The left plots report the task accuracy by each subgroup (denoting races) and average distance to decision boundary (right) of each subgroup. Note how the

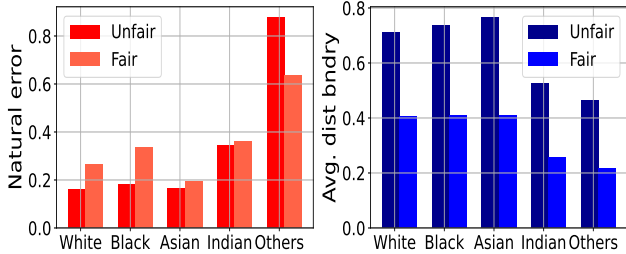


Figure 3. Comparison between group’s natural accuracy (left) and group’s average distance to the decision boundary (right) between unfair and fair models on the UTK-Face dataset.

fair classifier reduces the disparities in task accuracy experienced by the various subgroups. This effect, however, also reduces the *overall* average distance to the decision boundary. As a consequence, fair models will be more vulnerable to adversarial perturbations.

The next sections focus on assessing these theoretical intuitions onto general non-linear classifiers in a variety of settings and on devising a possible mitigation strategy to balance a good tradeoff between fairness and robustness.

## 7. Beyond the Linear Case

This section validates the theoretical intuitions presented above on much more complex architectures, datasets, and loss functions. The experiments focus on highlighting fairness, robustness, errors, and their relation to the distance to the decision boundary. When  $f_\theta$  is a non-linear model, computing the distance to the decision boundary becomes a computational challenge. Thus, this section uses a commonly adopted proxy metric that measures the difference between the first two order statistics of the softmax outputs in the model [21, 42].

**Datasets.** The experiments of this section focus on three vision datasets: *UTK-Face* [48], *FMNIST* [43] and *CIFAR-10* [20]. The adopted protected groups and labels in the UTK-Face datasets are *ethnicity* (White/Black/Indian/Asian/Others) or *age* (nine age bins), resulting in two distinct tasks. For FMNIST and CIFAR, the experiments use their standard labels and assume that labels are also protected groups, mirroring the setting of previous work [23, 39, 44]. A complete description of the dataset and settings is found in Appendix D.

**Settings.** The experiments consider several deep neural network architectures, including CNN [27], ResNet 50 [13] and VGG-13 [32]. The former uses 3 convolutional layers followed by 3 fully connected layers. Models trained on the UTK-Face data use a learning rate of  $1e^{-3}$  and 70 epochs. Those trained on FMNIST and CIFAR, use a learning rate of  $1e^{-1}$  and 200 epochs, as suggested in previous work [44]. For all datasets and models, unless otherwise

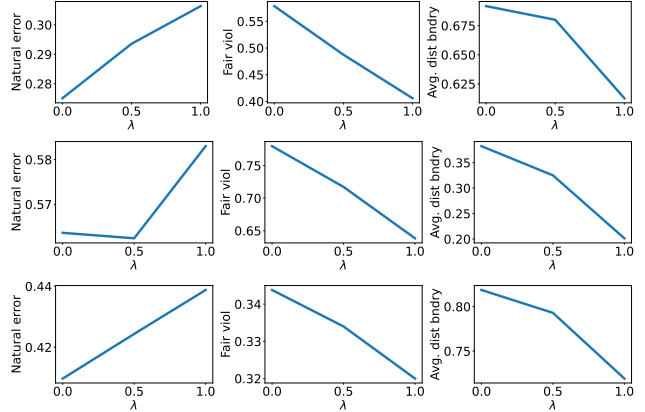


Figure 4. Natural errors, fairness violations, and average distance to the decision boundary for the UTK-Face *ethnicity* (top), UTK-Face *age bins* (middle) and CIFAR (bottom) datasets when varying the fairness parameter  $\lambda$  on a CNN model.

specified, a batch size of 32 is used. The experiments analyze penalty-based fairness method, RFGSM attacks [37], and the VGG-13 network, unless specified otherwise. Additional experiments using group-loss focused method (see Appendix B), additional network architectures, and adversarial attacks are reported in Appendix D.

### Fairness impacts on the decision boundary

As shown by Theorem 6.5, fairness reduces the average distance of the testing samples to the decision boundary. This section illustrates how this result carries over to larger non-linear models. Figure 4 reports results obtained by executing the penalty-based fair models on the UTK-Face datasets for ethnicity (top) and age (middle) classification and on CIFAR (bottom). A clear trend emerges: As more fairness is enforced (larger  $\lambda$  values), the natural errors (left plots) increase, while the fairness violations (center plots) decrease. Importantly, and in agreement with the theoretical results, the experiments report a sharp reduction to the average distance to the decision boundary (right plots). This behavior renders fair models more vulnerable to adversarial attacks, as will be highlighted shortly. Similar results are also observed for the group-loss based models and other architectures.

### Boundary errors increase as fairness decreases

This section highlights the key consequence of the sharp reduction to the average distance to the decision boundary: *the increase of the vulnerability to adversarial attacks*. Figure 5 (top) reports the natural errors (left), boundary errors (middle), and fairness violations (right) for a VGG-13 model trained on UTKFace dataset on the *ethnicity* task using a standard cross-entropy (CE) loss. Once again, other archi-

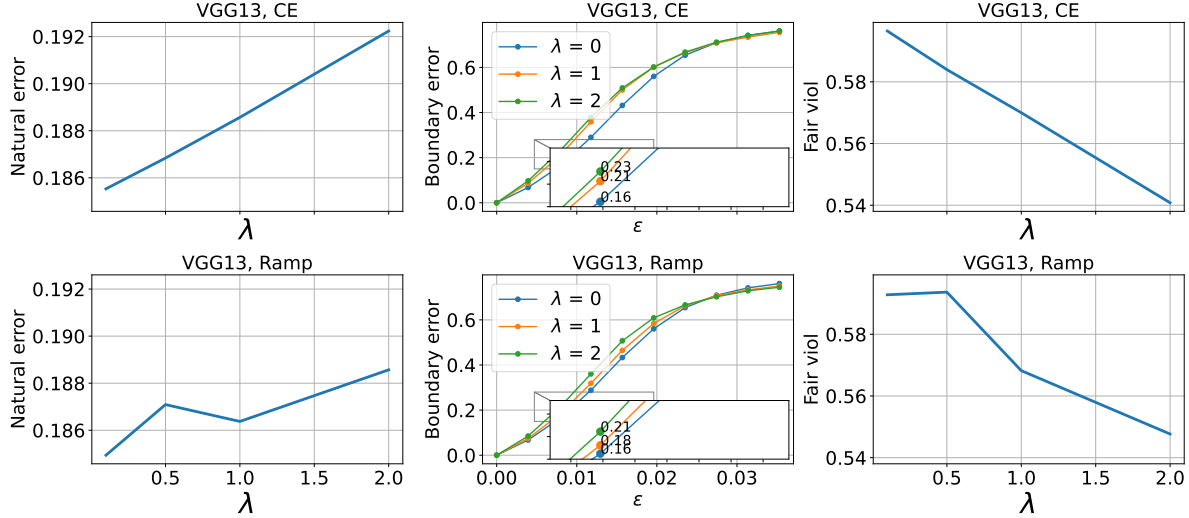


Figure 5. **Top:** Natural errors (left) and fairness violations (right) on the UTKFace *ethnicity* task at varying of the fairness parameters  $\lambda$ . The middle plots compares the robustness of fair ( $\lambda > 0$ ) vs. natural ( $\lambda = 0$ ) classifiers to different RFGSM attack levels. **Bottom:** Mitigating solution using the bounded Ramp loss.

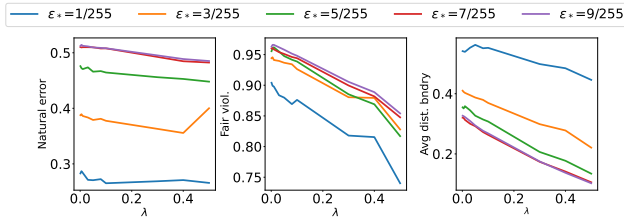


Figure 6. Natural error (left), fairness violation (middle) and average distance to the decision boundary (right) at varying of the margin perturbation  $\epsilon_*$  and fairness parameters  $\lambda$ .

tures<sup>1</sup> and datasets are reported in the appendix and the results follow the same trends as those reported here.

The natural errors and fairness violations are reported for *fair* classifiers, at varying of the fairness violation parameter  $\lambda$ . The boundary errors (middle) are reported for classifiers satisfying various fairness levels (i.e., using different  $\lambda$  values) and at varying of the strength  $\epsilon$  of the desired robustness level (see Equation (4)).

Notice how, compared to the natural models, the fair models incur much higher natural and boundary errors. In particular, the relative increase in boundary errors are significant: The fairness models have boundary errors that are up to 9% larger than their natural counterparts. These observations match the theoretical analysis and highlight a significant increase in vulnerability to adversarial examples by the fair models, even for moderate selections of the fairness violation

<sup>1</sup>With the caveat that VGG-13 could not be used for FMNIST since the 28x28 pixel resolution of FMNIST is smaller than that required by some VGG filters.

parameters  $\lambda$ .

### Enforcing Fairness and Robustness Simultaneously

This section considers an additional experiment to show how fairness may negatively impact robustness. It reports results of a classifier trying to enforce both fairness and robustness, similarly to the proposal of Xu et al. [44]. The resulting model aims at solving the following regularized ERM problem:

$$\min_{\theta} \frac{1}{n} \sum_{i=1}^n \max_{\|\tau\|_p \leq \epsilon_*} \ell(f_{\theta}(X_i + \tau), Y_i) + \lambda \left| \frac{1}{|D_c|} \sum_{(X,A,Y) \in D_c} \ell(f_{\theta}(X), Y) - \frac{1}{n} \sum_{i=1}^n \ell(f_{\theta}(X_i), Y_i) \right| \quad (9)$$

using stochastic gradient descent. The first component aims at increasing the robustness of the classifier under a margin perturbation  $\epsilon_*$ , following the PGD training [24] with perturbation norm  $p = \infty$ . It works by first generating adversarial samples  $X_i + \tau$ , where  $\|\tau\|_{\infty} \leq \epsilon_*$ , and then the learning progress aims at minimizing the loss between the model prediction for that adversarial samples and the ground-truth  $\ell(f_{\theta}(X_i + \tau), Y_i)$ . The larger the margin perturbation  $\epsilon_*$ , the more robust the resulting classifier. The second component implements a penalty-based fairness strategy [1], which promotes fairness by penalizing the difference among each groups' average loss and the overall's average loss.

The experiments vary the margin perturbation  $\epsilon_*$  (robustness) and the penalty value  $\lambda$  (fairness). Figure 6 reports the (natural) error (left), fairness violations (middle) and

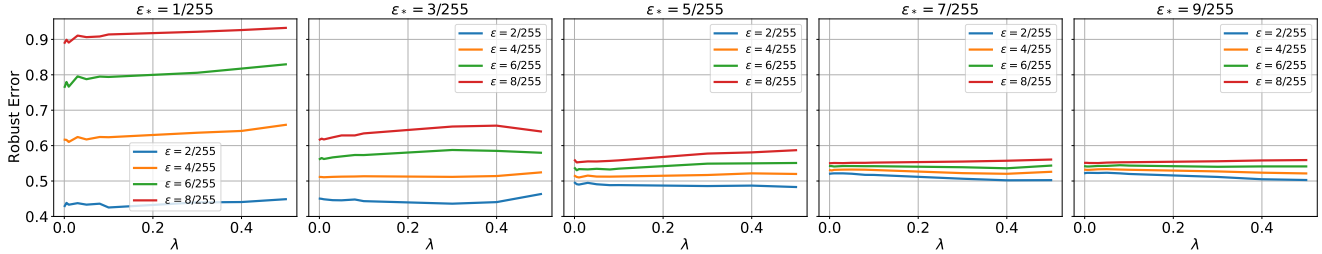


Figure 7. Robust errors for different attack levels  $\epsilon$  of a robust and fair classifier at varying of the margin perturbation  $\epsilon_*$  and fairness parameters  $\lambda$ .

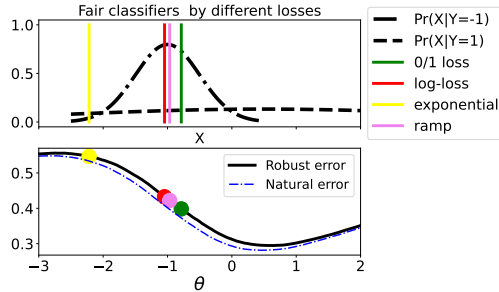


Figure 8. Classifiers obtained using different loss functions (top) and the associated natural and robust error obtained by such losses.

average distance to the decision boundary (right) for different levels of the margin perturbation  $\epsilon_*$  on the UTK-Face (ethnicity) dataset. As expected, enforcing larger margin perturbations  $\epsilon_*$  increases the average distance to the decision boundary (thus improving robustness), but at the cost of significantly increasing the natural errors. Increasing the fairness parameter  $\lambda$  decreases the average distance to the decision boundary).

Figure 7 reports the robust errors under different levels of adversarial attacks, which are specified by the level of perturbation  $\epsilon$ . Notice how the level of defense  $\epsilon_*$  correlates with higher robustness (and smaller average distances to the decision boundary) for all fairness parameters  $\lambda$  tested. These results show the challenge to achieving simultaneously robustness, fairness, and accuracy.

*Overall, the results show that, without a careful consideration, inducing a desired equity property on a learning task may create significant security challenges.* This should not be read as an endorsement to satisfy a single property, but as a call for additional research at the intersection of fairness and robustness in order to design appropriate tradeoffs.

## 8. A Mitigating Solution with Bounded Losses

While the previous sections have shown that the conflict between fairness and robustness is unavoidable, this section proposes a theoretically motivated solution attempting

to attenuate this tension. The proposed solution relies on the observation that, using standard (unbounded) loss functions, misclassified samples lying far away from the decision boundary are associated to much larger losses than those which are closer to it. Recall also that the decision boundary was found as the predominant factor linking fairness and robustness. This key observation suggests the use of a bounded loss function, defined as [7, 10]:

$$\ell_{Ramp}(f_\theta(X), Y) = \min(1, \max(0, 1 - Y f_\theta(X))).$$

and referred to as *Ramp loss*, with domain  $(0, 1]$ . The proposed strategy simply applies this loss function to a fair classifier (Equation 3). Its benefits can be appreciated in Figure 8, which reports the results for the same setting used in the previous section and compares a fair classifier trained using the ramp loss with one trained using a 0/1-loss (which is also bounded but not differentiable), a log-loss, and an exponential loss (both unbounded) (top). The results show that the fair classifier trained using a ramp-loss is the least impacted by misclassified samples, resulting in lower robust errors compared to unbounded losses. It can be observed in the bottom subplot, where its associated loss is the closest, among all differentiable losses, to the local minima. The observed benefits of the ramp loss also carry over high-dimensional data and non-linear models, as shown in Figure 5 bottom, and further reported in Appendix D.

## 9. Conclusions

This paper was motivated by two key challenges brought by the the adoption of modern machine learning systems in consequential domains: *fairness* and *robustness*. The paper observed and analyzed the relationship between these two important machine-learning properties and showed that fairness increases vulnerability to adversarial examples. Through a theoretical analysis on linear models, this work provided a new understanding of why such tension arises and identified the distance to the decision boundary as a key explanation factor linking fairness and robustness. These theoretical findings were validated on non-linear models through extensive experiments on a variety of vision tasks. Finally, building



from this new understanding, the paper proposed a simple, yet effective, strategy to find a better balance between accuracy, fairness and robustness. We hope these results could stimulate a needed discussion and research at the intersection of fairness and robustness to achieve appropriate tradeoffs.

## Acknowledgments

This research is partially supported by grants NSF-2112533, NSF-2133169 and NSF-2143706. F. Fioretto is also supported by a Google Research Scholar Award and an Amazon Research Award. Its views and conclusions are those of the authors only.

## References

- [1] Alekh Agarwal, Alina Beygelzimer, Miroslav Dudík, John Langford, and Hanna Wallach. A reductions approach to fair classification. In *International Conference on Machine Learning*, pages 60–69. PMLR, 2018. 2, 7
- [2] Eugene Bagdasaryan, Omid Poursaeed, and Vitaly Shmatikov. Differential privacy has disparate impact on model accuracy. *Advances in neural information processing systems*, 32, 2019. 2
- [3] Joy Buolamwini and Timnit Gebru. Gender shades: Intersectional accuracy disparities in commercial gender classification. In *Conference on fairness, accountability and transparency*, pages 77–91. PMLR, 2018. 2
- [4] Robin Burke. Hybrid systems for personalized recommendations. In *IJCAI Workshop on Intelligent Techniques for Web Personalization*, pages 133–152. Springer, 2003. 1
- [5] Simon Caton and Christian Haas. Fairness in machine learning: A survey. *arXiv preprint arXiv:2010.04053*, 2020. 2
- [6] Jin-A Choi and Kiho Lim. Identifying machine learning techniques for classification of target advertising. *ICT Express*, 6(3):175–180, 2020. 1
- [7] Ronan Collobert, Fabian Sinz, Jason Weston, and Léon Bottou. Trading convexity for scalability. In *Proceedings of the 23rd international conference on Machine learning*, pages 201–208, 2006. 8, 17
- [8] Sorelle A Friedler, Carlos Scheidegger, Suresh Venkatasubramanian, Sonam Choudhary, Evan P Hamilton, and Derek Roth. A comparative study of fairness-enhancing interventions in machine learning. In *Proceedings of the conference on fairness, accountability, and transparency*, pages 329–338, 2019. 2
- [9] Angus Galloway, Anna Golubeva, Thomas Tanay, Medhat Moussa, and Graham W Taylor. Batch normalization is a cause of adversarial vulnerability. *arXiv preprint arXiv:1905.02161*, 2019. 2
- [10] Gabriel Goh, Andrew Cotter, Maya Gupta, and Michael P Friedlander. Satisfying real-world goals with dataset constraints. *Advances in Neural Information Processing Systems*, 29, 2016. 8, 17
- [11] Ian J Goodfellow, Jonathon Shlens, and Christian Szegedy. Explaining and harnessing adversarial examples. *arXiv preprint arXiv:1412.6572*, 2014. 2
- [12] Trevor Hastie, Robert Tibshirani, Jerome H Friedman, and Jerome H Friedman. *The elements of statistical learning: data mining, inference, and prediction*, volume 2. Springer, 2009. 17
- [13] Kaiming He, Xiangyu Zhang, Shaoqing Ren, and Jian Sun. Deep residual learning for image recognition. In *Proceedings of the IEEE conference on computer vision and pattern recognition*, pages 770–778, 2016. 6, 15
- [14] Sara Hooker, Yann Dauphin, Aaron Courville, and Andrea Frome. Selective brain damage: Measuring the disparate impact of model pruning. 2019. 2
- [15] Sara Hooker, Nyalleng Moorosi, Gregory Clark, Samy Bengio, and Emily Denton. Characterising bias in compressed models. *arXiv preprint arXiv:2010.03058*, 2020. 2
- [16] Senerath Mudalige Don Alexis Chinthaka Jayatilake and Gamage Upeksha Ganegoda. Involvement of machine learning tools in healthcare decision making. *Journal of Healthcare Engineering*, 2021, 2021. 1
- [17] Fereshte Khani and Percy Liang. Feature noise induces loss discrepancy across groups. In *International Conference on Machine Learning*, pages 5209–5219. PMLR, 2020. 2
- [18] Hoki Kim. Torchattacks: A pytorch repository for adversarial attacks. *arXiv preprint arXiv:2010.01950*, 2020. 16
- [19] Anoop Krishnan, Ali Almadan, and Ajita Rattani. Understanding fairness of gender classification algorithms across gender-race groups. In *2020 19th IEEE International Conference on Machine Learning and Applications (ICMLA)*, pages 1028–1035. IEEE, 2020. 2
- [20] Alex Krizhevsky, Geoffrey Hinton, et al. Learning multiple layers of features from tiny images. 2009. 6, 15
- [21] Mathias Lecuyer, Vaggelis Atlidakis, Roxana Geambasu, Daniel Hsu, and Suman Jana. Certified robustness to adversarial examples with differential privacy. In *2019 IEEE Symposium on Security and Privacy (SP)*, pages 656–672. IEEE, 2019. 6
- [22] Tian Li, Maziar Sanjabi, Ahmad Beirami, and Virginia Smith. Fair resource allocation in federated learning. *arXiv preprint arXiv:1905.10497*, 2019. 15
- [23] Xinsong Ma, Zekai Wang, and Weiwei Liu. On the trade-off between robustness and fairness. *Advances in Neural Information Processing Systems*, 35, 2022. 6
- [24] Aleksander Madry, Aleksandar Makelov, Ludwig Schmidt, Dimitris Tsipras, and Adrian Vladu. Towards deep learning models resistant to adversarial attacks. *arXiv preprint arXiv:1706.06083*, 2017. 7, 16
- [25] Ninareh Mehrabi, Fred Morstatter, Nripsuta Saxena, Kristina Lerman, and Aram Galstyan. A survey on bias and fairness in machine learning. *ACM Computing Surveys (CSUR)*, 54(6):1–35, 2021. 1, 2
- [26] Vedant Nanda, Samuel Dooley, Sahil Singla, Soheil Feizi, and John P Dickerson. Fairness through robustness: Investigating robustness disparity in deep learning. In *Proceedings of the 2021 ACM Conference on Fairness, Accountability, and Transparency*, pages 466–477, 2021. 2
- [27] Keiron O’Shea and Ryan Nash. An introduction to convolutional neural networks. *arXiv preprint arXiv:1511.08458*, 2015. 6

- [28] Inioluwa Deborah Raji, Timnit Gebru, Margaret Mitchell, Joy Buolamwini, Joonseok Lee, and Emily Denton. Saving face: Investigating the ethical concerns of facial recognition auditing. In *Proceedings of the AAAI/ACM Conference on AI, Ethics, and Society*, pages 145–151, 2020. 4
- [29] Kit T Rodolfa, Hemank Lamba, and Rayid Ghani. Empirical observation of negligible fairness–accuracy trade-offs in machine learning for public policy. *Nature Machine Intelligence*, 3(10):896–904, 2021. 1
- [30] Candice Schumann, Jeffrey Foster, Nicholas Mattei, and John Dickerson. We need fairness and explainability in algorithmic hiring. In *International Conference on Autonomous Agents and Multi-Agent Systems (AAMAS)*, 2020. 1
- [31] Adi Shamir, Itay Safran, Eyal Ronen, and Orr Dunkelman. A simple explanation for the existence of adversarial examples with small hamming distance. *arXiv preprint arXiv:1901.10861*, 2019. 2
- [32] Karen Simonyan and Andrew Zisserman. Very deep convolutional networks for large-scale image recognition. *arXiv preprint arXiv:1409.1556*, 2014. 6, 15
- [33] Alexander Stevens, Peter Deruyck, Ziboud Van Veldhoven, and Jan Vanthienen. Explainability and fairness in machine learning: Improve fair end-to-end lending for kiva. In *2020 IEEE Symposium Series on Computational Intelligence (SSCI)*, pages 1241–1248. IEEE, 2020. 1
- [34] Shivashankar Subramanian, Afshin Rahimi, Timothy Baldwin, Trevor Cohn, and Lea Frermann. Fairness-aware class imbalanced learning. *arXiv preprint arXiv:2109.10444*, 2021. 2
- [35] Rhea Sukthanker, Samuel Dooley, John P Dickerson, Colin White, Frank Hutter, and Micah Goldblum. On the importance of architectures and hyperparameters for fairness in face recognition. *arXiv preprint arXiv:2210.09943*, 2022. 2
- [36] Christian Szegedy, Wojciech Zaremba, Ilya Sutskever, Joan Bruna, Dumitru Erhan, Ian Goodfellow, and Rob Fergus. Intriguing properties of neural networks. *arXiv preprint arXiv:1312.6199*, 2013. 2
- [37] Florian Tramèr, Alexey Kurakin, Nicolas Papernot, Ian Goodfellow, Dan Boneh, and Patrick McDaniel. Ensemble adversarial training: Attacks and defenses. *arXiv preprint arXiv:1705.07204*, 2017. 3, 6, 16
- [38] Cuong Tran, My Dinh, and Ferdinando Fioretto. Differentially private empirical risk minimization under the fairness lens. In *Advances in Neural Information Processing Systems*, 2021. 2
- [39] Cuong Tran, Ferdinando Fioretto, Jung-Eun Kim, and Rakshit Naidu. Pruning has a disparate impact on model accuracy. In *Advances in Neural Information Processing Systems (NeurIPS)*, 2022. 2, 6
- [40] Cuong Tran, Ferdinando Fioretto, and Pascal Van Hentenryck. Differentially private and fair deep learning: A lagrangian dual approach. In *Proceedings of the AAAI Conference on Artificial Intelligence*, volume 35, pages 9932–9939, 2021. 2
- [41] Haohan Wang, Xindi Wu, Zeyi Huang, and Eric P Xing. High-frequency component helps explain the generalization of convolutional neural networks. In *Proceedings of the IEEE/CVF Conference on Computer Vision and Pattern Recognition*, pages 8684–8694, 2020. 2
- [42] Ziqi Wang and Marco Loog. Enhancing classifier conservativeness and robustness by polynomiality. In *Proceedings of the IEEE/CVF Conference on Computer Vision and Pattern Recognition*, pages 13327–13336, 2022. 6
- [43] Han Xiao, Kashif Rasul, and Roland Vollgraf. Fashion-mnist: a novel image dataset for benchmarking machine learning algorithms. *arXiv preprint arXiv:1708.07747*, 2017. 6, 15
- [44] Han Xu, Xiaorui Liu, Yaxin Li, Anil Jain, and Jiliang Tang. To be robust or to be fair: Towards fairness in adversarial training. In *International Conference on Machine Learning*. PMLR, 2021. 2, 6, 7
- [45] Xingkun Xu, Yuge Huang, Pengcheng Shen, Shaoxin Li, Jilin Li, Feiyue Huang, Yong Li, and Zhen Cui. Consistent instance false positive improves fairness in face recognition. In *Proceedings of the IEEE/CVF conference on computer vision and pattern recognition*, pages 578–586, 2021. 2
- [46] Zhewei Yao, Amir Gholami, Qi Lei, Kurt Keutzer, and Michael W Mahoney. Hessian-based analysis of large batch training and robustness to adversaries. *arXiv preprint arXiv:1802.08241*, 2018. 2
- [47] Hongyang Zhang, Yaodong Yu, Jiantao Jiao, Eric Xing, Laurent El Ghaoui, and Michael Jordan. Theoretically principled trade-off between robustness and accuracy. In *International conference on machine learning*, pages 7472–7482. PMLR, 2019. 3
- [48] Zhifei Zhang, Yang Song, and Hairong Qi. Age progression/regression by conditional adversarial autoencoder. In *IEEE Conference on Computer Vision and Pattern Recognition (CVPR)*. 6, 15
- [49] Han Zhao and Geoff Gordon. Inherent tradeoffs in learning fair representations. *Advances in neural information processing systems*, 32:15675–15685, 2019. 2

## A. Missing Proofs

### Proof of Theorem 6.1

*Proof.* i) Notice that the natural classification error and its derivative can be expressed as

$$\begin{aligned}\mathcal{L}_\theta^{\text{nat}} &= \Pr(f_\theta(X) \neq Y) \\ &= \frac{1}{2} \Pr(f_\theta(X) \neq 1 \mid Y = 1) + \\ &\quad \frac{1}{2} \Pr(f_\theta(X) \neq -1 \mid Y = -1) \\ &= \frac{1}{2} \int_{-\infty}^{\theta} \frac{1}{\sqrt{2\pi}K} \exp\left(-\frac{(x - \mu_+)^2}{2K^2}\right) dx + \\ &\quad \frac{1}{2} \int_{\theta}^{+\infty} \frac{1}{\sqrt{2\pi}} \exp\left(-\frac{(x - \mu_-)^2}{2}\right) dx.\end{aligned}$$

and

$$(\mathcal{L}_\theta^{\text{nat}})' = \frac{\left[\exp\left(-\frac{(\theta - \mu_+)^2}{2K^2}\right) - K \exp\left(-\frac{(\theta - \mu_-)^2}{2}\right)\right]}{2K\sqrt{2\pi}}.$$

The derivative  $(\mathcal{L}_\theta^{\text{nat}})'$  turns out to be an increasing function over the interval  $[\mu_-, \mu_+]$  with  $(\mathcal{L}_{\mu_-}^{\text{nat}})' < 0$  and  $(\mathcal{L}_{\mu_+}^{\text{nat}})' > 0$  due to the assumption that  $K < B_K < \exp\left(-\frac{(\mu_+ - \mu_-)^2}{2}\right)$ .

Since the Bayes classifier is to minimize the natural classification error,  $\theta$  is supposed to be the unique root of  $(\mathcal{L}_\theta^{\text{nat}})'$ , i.e.,

$$\frac{\left[\exp\left(-\frac{(\dot{\theta} - \mu_+)^2}{2K^2}\right) - K \exp\left(-\frac{(\dot{\theta} - \mu_-)^2}{2}\right)\right]}{2K\sqrt{2\pi}} = 0.$$

By solving the equation above, we end up with the following.

$$\begin{aligned}\dot{\theta} &= \mu_- - \frac{\mu_+ - \mu_-}{K^2 - 1} + \\ &\quad \frac{K}{K^2 - 1} \sqrt{2(K^2 - 1) \ln(K) + (\mu_+ - \mu_-)^2},\end{aligned}$$

which belongs to the open interval  $(\mu_-, \mu_+)$ .

ii) Equalized classification errors require the following equations hold.

$$\begin{aligned}&\Pr(f_{\theta_f}(X) \neq 1 \mid Y = 1) \\ &= \int_{-\infty}^{\theta_f} \frac{1}{\sqrt{2\pi}K} \exp\left(-\frac{(x - \mu_+)^2}{2K^2}\right) dx \\ &= \int_{\theta_f}^{+\infty} \frac{1}{\sqrt{2\pi}} \exp\left(-\frac{(x - \mu_-)^2}{2}\right) dx \\ &= \Pr(f_{\theta_f}(X) \neq -1 \mid Y = -1),\end{aligned}$$

which leads to the result that

$$\theta_f = \mu_- + \frac{\mu_+ - \mu_-}{K + 1} > \mu_- + \epsilon,$$

where the inequality is due to the assumption that  $K < (\mu_+ - \mu_-)/\epsilon - 1 \leq B_K$ .

iii) The robust classification error and its partial derivative can then be given by the following:

$$\begin{aligned}\mathcal{L}_\theta^{\text{rob}}(\epsilon) &= \Pr(\exists |\tau| \leq \epsilon, f_\theta(X + \tau) \neq Y) \\ &= \frac{1}{2} \Pr(\exists |\tau| \leq \epsilon, f_\theta(X + \tau) \neq 1 \mid Y = 1) + \\ &\quad \frac{1}{2} \Pr(\exists |\tau| \leq \epsilon, f_\theta(X + \tau) \neq -1 \mid Y = -1) \\ &= \frac{1}{2} (\Pr(X \leq \theta + \epsilon \mid Y = 1) + \Pr(X > \theta - \epsilon \mid Y = -1)) \\ &= \frac{1}{2} \int_{-\infty}^{\theta + \epsilon} \frac{1}{\sqrt{2\pi}K} \exp\left(-\frac{(x - \mu_+)^2}{2K^2}\right) dx + \\ &\quad \frac{1}{2} \int_{\theta - \epsilon}^{+\infty} \frac{1}{\sqrt{2\pi}} \exp\left(-\frac{(x - \mu_-)^2}{2}\right) dx,\end{aligned}$$

and

$$\begin{aligned}\frac{\partial}{\partial \theta} \mathcal{L}_\theta^{\text{rob}}(\epsilon) &= \\ &\frac{\left[\exp\left(-\frac{(\theta + \epsilon - \mu_+)^2}{2K^2}\right) - K \exp\left(-\frac{(\theta - \epsilon - \mu_-)^2}{2}\right)\right]}{2K\sqrt{2\pi}}.\end{aligned}\tag{10}$$

By the assumptions made about  $K$  and  $\epsilon$ , there exists a unique root  $\theta_r^{(\epsilon)} \in (\mu_-, \mu_+ - \epsilon)$  of  $\frac{\partial}{\partial \theta} \mathcal{L}_\theta^{\text{rob}}(\epsilon) = 0$  such that the robust error  $\mathcal{L}_\theta^{\text{rob}}(\epsilon)$  is decreasing over  $(\mu_-, \theta_r^{(\epsilon)})$  while increasing over  $(\theta_r^{(\epsilon)}, \mu_+)$ , i.e.,

$$\frac{\partial}{\partial \theta} \mathcal{L}_\theta^{\text{rob}}(\epsilon) \begin{cases} < 0, & \theta \in (\mu_-, \theta_r^{(\epsilon)}), \\ > 0, & \theta \in (\theta_r^{(\epsilon)}, \mu_+), \end{cases}\tag{11}$$

which indicates that  $\theta_r^{(\epsilon)}$  essentially minimizes the robust classification error.

Therefore, by solving  $\frac{\partial}{\partial \theta} \mathcal{L}_\theta^{\text{rob}}(\epsilon) \Big|_{\theta = \theta_r^{(\epsilon)}} = 0$ , we are able to derive the robust classifier as follows.

$$\begin{aligned}\theta_r^{(\epsilon)} &= \mu_- - \frac{\mu_+ - \mu_- - (K^2 + 1)\epsilon}{K^2 - 1} + \\ &\quad \frac{K}{K^2 - 1} \sqrt{2(K^2 - 1) \ln(K) + (\mu_+ - \mu_- - 2\epsilon)^2},\end{aligned}$$

which satisfies the following

$$\theta_r^{(\epsilon)} \leq \mu_+ - \epsilon \leq \mu_+.$$

iv) The next step is to compare the three different classifiers we just obtained. We start with the Bayes and fair classifiers.

$$\begin{aligned}
& \hat{\theta} - \theta_f \\
&= \frac{K \left( \sqrt{2(K^2 - 1) \ln(K)} + (\mu_+ - \mu_-)^2 - \mu_+ - \mu_- \right)}{K^2 - 1} \\
&> \frac{K \left( \sqrt{(\mu_+ - \mu_-)^2} - \mu_+ - \mu_- \right)}{K^2 - 1} \\
&= 0,
\end{aligned}$$

where the inequality comes from the assumption that  $K$  is strictly larger than 1. It indicates that the threshold of the Bayes classifier is greater than that of the fair classifier. Then, we move on to the comparison between the Bayes and robust classifier. Note that the robust classifier is identical to the Bayes classifier when  $\epsilon$  is 0, i.e.,  $\theta_r^{(0)} = \hat{\theta}$ . Besides, we have that

$$\begin{aligned}
\frac{\partial}{\partial \epsilon} \theta_r^{(\epsilon)} &= \frac{K^2 + 1 - \frac{2(\mu_+ - \mu_- - 2\epsilon)K}{\sqrt{(\mu_+ - \mu_- - 2\epsilon)^2 + 2(K^2 - 1) \ln(K)}}}{K^2 - 1} \\
&> \frac{K^2 + 1 - \frac{2(\mu_+ - \mu_- - 2\epsilon)K}{\sqrt{(\mu_+ - \mu_- - 2\epsilon)^2}}}{K^2 - 1} \quad (12)
\end{aligned}$$

$$\begin{aligned}
&= \frac{K^2 - 2k + 1}{K^2 - 1} \quad (13) \\
&= \frac{K - 1}{K + 1} > 0,
\end{aligned}$$

where Equation (12) is due to the fact that  $K > 1$  and Equation (13) comes from the assumption that  $\epsilon \leq \frac{\mu_+ - \mu_-}{2}$ , which ensures that  $\mu_+ - \mu_- - 2\epsilon$  is strictly positive. Therefore, the partial derivative of  $\theta_r^{(\epsilon)}$  in  $\epsilon$  is strictly positive over the interval  $\left[0, \frac{\mu_+ - \mu_-}{2}\right]$ . As a consequence, for any  $\epsilon \in \left[0, \frac{\mu_+ - \mu_-}{2}\right]$ , the following relation always holds that  $\mu_+ \geq \theta_r^{(\epsilon)} \geq \theta_r^{(0)} = \hat{\theta}$ . Putting things together, we end up with following relation: for any  $\epsilon \in \left[0, \frac{\mu_+ - \mu_-}{2}\right]$  and  $K \in (1, B_K)$ ,

$$\mu_- + \epsilon \leq \theta_f \leq \hat{\theta} \leq \theta_r^{(\epsilon)} \leq \mu_+ - \epsilon.$$

□

### Proof of Corollary 6.2

*Proof.* Note that, by Equation (11), the robust classification error is strictly decreasing over  $(\mu_-, \theta_r^{(\epsilon)})$ . Then, by Equation (8) in Proposition 6.1, the three classifiers satisfy the following relation

$$\mu_- \leq \theta_f \leq \hat{\theta} \leq \theta_r^{(\epsilon)}.$$

Due to contiguity of  $\mathcal{L}_\theta^{\text{rob}}(\epsilon)$ , we can argue that, for any  $\epsilon \in \left(0, \frac{\mu_+ - \mu_-}{2}\right)$  and  $K \in (1, B_K)$ ,

$$\mathcal{L}_{\theta_f}^{\text{rob}}(\epsilon) \geq \mathcal{L}_{\hat{\theta}}^{\text{rob}}(\epsilon) \geq \mathcal{L}_{\theta_r^{(\epsilon)}}^{\text{rob}}(\epsilon).$$

□

### Proof of Corollary 6.3

*Proof.* The boundary error and its partial derivative are presented in the following:

$$\begin{aligned}
& \mathcal{L}_\theta^{\text{bdy}}(\epsilon) \\
&= \Pr(\exists |\tau| \leq \epsilon, f_\theta(X + \tau) \neq Y, f_\theta(X) = Y) \\
&= \frac{1}{2} \Pr(\exists |\tau| \leq \epsilon, f_\theta(X + \tau) = -1, f_\theta(X) = 1 \mid Y = 1) + \\
&\quad \frac{1}{2} \Pr(\exists |\tau| \leq \epsilon, f_\theta(X + \tau) = 1, f_\theta(X) = -1 \mid Y = -1) \\
&= \frac{1}{2} \Pr(\theta < X \leq \theta + \epsilon \mid Y = 1) + \\
&\quad \frac{1}{2} \Pr(\theta \geq X > \theta - \epsilon \mid Y = -1) \\
&= \frac{1}{2} \int_\theta^{\theta + \epsilon} \frac{1}{\sqrt{2\pi}K} \exp\left(-\frac{(x - \mu_+)^2}{2K^2}\right) dx + \\
&\quad \frac{1}{2} \int_{\theta - \epsilon}^\theta \frac{1}{\sqrt{2\pi}} \exp\left(-\frac{(x - \mu_-)^2}{2}\right) dx,
\end{aligned}$$

and

$$\begin{aligned}
& \frac{\partial}{\partial \theta} \mathcal{L}_\theta^{\text{bdy}}(\epsilon) \\
&= \frac{\exp\left(-\frac{(\theta + \epsilon - \mu_+)^2}{2K^2}\right)}{2\sqrt{2\pi}K} - \frac{\exp\left(-\frac{(\theta - \mu_+)^2}{2K^2}\right)}{2\sqrt{2\pi}K} + \\
&\quad \frac{\exp\left(-\frac{(\theta - \mu_-)^2}{2}\right)}{2\sqrt{2\pi}} - \frac{\exp\left(-\frac{(\theta - \epsilon - \mu_-)^2}{2}\right)}{2\sqrt{2\pi}} \\
&= \frac{g(\epsilon; \theta, K) - g(0; \theta, K)}{2\sqrt{2\pi}},
\end{aligned}$$

where  $g: \mathbb{R} \mapsto \mathbb{R}$  is an auxiliary function shown as follows

$$\begin{aligned}
& g(\epsilon; \theta, K) := \\
& \frac{\exp\left(-\frac{(\theta + \epsilon - \mu_+)^2}{2K^2}\right)}{K} - \exp\left(-\frac{(\theta - \epsilon - \mu_-)^2}{2}\right). \quad (14)
\end{aligned}$$

By Proposition A.1, the partial derivative of the boundary error in  $\theta$  is always negative for any  $\theta \in \left[\theta_f, \theta_r^{(\epsilon)}\right]$  because

$$\frac{\partial}{\partial \theta} \mathcal{L}_\theta^{\text{bdy}}(\epsilon) = \frac{g(\epsilon; \theta, K) - g(0; \theta, K)}{2\sqrt{2\pi}} < 0.$$



It leads to the following result that the boundary error  $\mathcal{L}_\theta^{\text{rob}}(\epsilon)$  decreases in  $\theta$  over  $[\theta_f, \theta_r^{(\epsilon)}]$ , and, therefore,

$$\mathcal{L}_{\theta_f}^{\text{bdy}}(\epsilon) \geq \mathcal{L}_\theta^{\text{bdy}}(\epsilon) \geq \mathcal{L}_{\theta_r^{(\epsilon)}}^{\text{bdy}}(\epsilon).$$

□

**Proposition A.1.** For any  $\epsilon \in [0, \frac{\mu_+ - \mu_-}{4}]$ ,  $K \in (1, \bar{B}_K)$ , and  $\theta \in [\theta_f, \theta_r^{(\epsilon)}]$ , the following relation holds

$$g(\epsilon; \theta, K) \leq g(0; \theta, K), \quad (15)$$

where the function  $g$  is defined in Equation (14).

*Proof.* Note that the partial derivative of the function  $g$  in  $\epsilon$  can be given by

$$\begin{aligned} \frac{\partial}{\partial \epsilon} g(\epsilon; \theta, K) &= \frac{\mu_+ - \theta - \epsilon}{K^3} \exp\left(-\frac{(\mu_+ - \theta - \epsilon)^2}{2K^2}\right) - \\ &\quad (\theta - \epsilon - \mu_-) \exp\left(-\frac{(\theta - \epsilon - \mu_-)^2}{2}\right). \end{aligned}$$

In order to establish the result in Equation (15), it suffices to demonstrate that the partial derivative  $\frac{\partial}{\partial \epsilon} g(\epsilon; \theta, K)$  is negative, which implies that the function  $g(\epsilon; \theta, K)$  is strictly decreasing over  $[0, \frac{\mu_+ - \mu_-}{4}]$ . Note that

$$\begin{aligned} &\ln\left(\frac{\mu_+ - \theta - \epsilon}{K^3} \exp\left(-\frac{(\mu_+ - \theta - \epsilon)^2}{2K^2}\right)\right) - \\ &\ln\left((\theta - \epsilon - \mu_-) \exp\left(-\frac{(\theta - \epsilon - \mu_-)^2}{2}\right)\right) \\ &= -[\ln(\theta - \epsilon - \mu_-) - \ln(\mu_+ - \theta - \epsilon)] + \\ &\quad \left[\frac{(\theta - \epsilon - \mu_-)^2}{2} - \frac{(\mu_+ - \theta - \epsilon)^2}{2K^2}\right] - 3\ln(K) \\ &= \frac{1}{2}(q(\theta; \epsilon, K) - p(\theta; \epsilon, K) - 4\ln(K)) \\ &\leq 0, \end{aligned}$$

where the last inequality comes from Proposition A.2. It follows that, due to monotonicity of the function  $x \mapsto \ln(x)$ ,

$$\begin{aligned} \frac{\partial}{\partial \epsilon} g(\epsilon; \theta, K) &= \frac{\mu_+ - \theta - \epsilon}{K^3} \exp\left(-\frac{(\mu_+ - \theta - \epsilon)^2}{2K^2}\right) - \\ &\quad (\theta - \epsilon - \mu_-) \exp\left(-\frac{(\theta - \epsilon - \mu_-)^2}{2}\right) \\ &\leq 0, \end{aligned}$$

which completes our proof here. □

**Proposition A.2.** For any  $\epsilon \in [0, \frac{\mu_+ - \mu_-}{4}]$ ,  $K \in (1, \bar{B}_K)$ , and  $\theta \in [\theta_f, \theta_r^{(\epsilon)}]$ , the following relation always holds:

$$p(\theta; \epsilon, K) \geq q(\theta; \epsilon, K) - 4\ln(K),$$

where

$$p(\theta; \epsilon, K) = \ln((\theta - \epsilon - \mu_-)^2) - \ln\left(\frac{(\mu_+ - \theta - \epsilon)^2}{K^2}\right), \quad (16)$$

$$q(\theta; \epsilon, K) = (\theta - \epsilon - \mu_-)^2 - \frac{(\mu_+ - \theta - \epsilon)^2}{K^2}. \quad (17)$$

*Proof.* First off, observe that the functions  $p$  and  $q$  are both increasing over  $[\theta_f, \theta_r^{(\epsilon)}]$ . It follows that, for any  $[\theta_f, \theta_r^{(\epsilon)}]$ ,

$$p(\theta; \epsilon, K) \geq p(\theta_f; \epsilon, K) \quad (18)$$

$$\geq -2\ln(K) = 2\ln(K) - 4\ln(K) \quad (19)$$

$$= q(\theta_r^{(\epsilon)}; \epsilon, K) - 4\ln(K) \quad (20)$$

$$\geq q(\theta; \epsilon, K) - 4\ln(K), \quad (21)$$

where Equation (18) and (21) come from monotonicity of the functions  $p$  and  $q$ . Equation (19) and (20) are due to Proposition A.4 and A.3 respectively. □

**Proposition A.3.** For any  $\epsilon \in [0, \frac{\mu_+ - \mu_-}{4}]$  and  $K \in (1, \bar{B}_K)$ ,

$$q(\theta_r^{(\epsilon)}; \epsilon, K) = 2\ln(K),$$

where the definition of the function  $q$  is given in Equation (17).

*Proof.* Due to optimality of  $\theta_r^{(\epsilon)}$  in terms of robust error,  $\theta_r^{(\epsilon)}$  should be a solution to Equation (10), i.e.,

$$\begin{aligned} &\exp\left(-\frac{(\theta_r^{(\epsilon)} + \epsilon - \mu_+)^2}{2K^2}\right) - \\ &\quad K \exp\left(-\frac{(\theta_r^{(\epsilon)} - \epsilon - \mu_-)^2}{2}\right) = 0, \end{aligned}$$

which leads to the following, by multiplying the both sides with the term  $\exp\left(\frac{(\theta_r^{(\epsilon)} - \epsilon - \mu_-)^2}{2}\right)$ ,

$$\exp\left(\frac{q(\theta_r^{(\epsilon)}; \epsilon, K)}{2}\right) = K,$$

and

$$q(\theta_r^{(\epsilon)}; \epsilon, K) = 2\ln(K). \quad \square$$

**Proposition A.4.** For any  $\epsilon \in [0, \frac{\mu_+ - \mu_-}{4}]$  and  $K \in (1, \bar{B}_K)$ ,

$$p(\theta_f; \epsilon, K) \geq -2\ln(K), \quad (22)$$

where the definition of the function  $p$  is given in Equation (16).

*Proof.* Equation (22) can be rewritten into the following equivalent form

$$\exp(p(\theta_f; \epsilon, K) + 2 \ln(K)) = K - \frac{(K-1)\epsilon}{\frac{\mu_+ - \mu_-}{K+1} - \frac{\epsilon}{K}} > 1. \quad (23)$$

Note that

$$\begin{aligned} K \leq \bar{B}_K &\implies K + \frac{1}{K} \leq \frac{\mu_+ - \mu_-}{\epsilon} - 2 \\ &\implies \frac{\mu_+ - \mu_-}{K+1} \geq \frac{K+1}{K}\epsilon, \end{aligned}$$

which leads to the following result

$$\begin{aligned} &\exp(p(\theta_f; \epsilon, K) + 2 \ln(K)) \\ &= K - \frac{(K-1)\epsilon}{\frac{\mu_+ - \mu_-}{K+1} - \frac{\epsilon}{K}} \geq K - (K-1) \\ &= 1. \end{aligned}$$

It helps complete our proof here.  $\square$

#### Proof of Theorem 6.4

*Proof.* Since  $f_\theta$  is essentially a linear classifier, the distance to the decision boundary of  $f_\theta$  is simply the absolute value between the feature  $X$  and the threshold  $\theta$ , i.e.,  $\Delta(X, f_\theta) = |X - \theta|$ . Notice that the average distance to the decision boundary of  $f_\theta$  can then be given by

$$\begin{aligned} \mathbb{E}[\Delta(X, f_\theta)] &= \mathbb{E}[|X - \theta|] \\ &= \mathbb{E}[|X - \theta| \mid Y = 1] \cdot \Pr(Y = 1) + \\ &\quad \mathbb{E}[|X - \theta| \mid Y = -1] \cdot \Pr(Y = -1) \\ &= \frac{1}{2} \int_{-\infty}^{+\infty} \frac{|x - \theta|}{\sqrt{2\pi}K} \exp\left(-\frac{(x - \mu_+)^2}{2K^2}\right) dx + \\ &\quad \frac{1}{2} \int_{-\infty}^{+\infty} \frac{|x - \theta|}{\sqrt{2\pi}} \exp\left(-\frac{(x - \mu_-)^2}{2}\right) dx, \end{aligned}$$

whose derivative can be expressed as

$$(\mathbb{E}[\Delta(X, f_\theta)])' = 2 \left( \Phi(\theta - \mu_-) - \Phi\left(\frac{\mu_+ - \theta}{K}\right) \right),$$

where  $\Phi$  represents the cumulative distribution function associated with the standard normal distribution. Recall that

$$\theta_f = \mu_- + \frac{\mu_+ - \mu_-}{K+1}.$$

It follows that

$$(\mathbb{E}[\Delta(X, f_\theta)])' \begin{cases} < 0, & \theta \in (\mu_-, \theta_f), \\ > 0, & \theta \in (\theta_f, \mu_+), \end{cases}$$

which implies that the average distance strictly decreases over  $(\mu_-, \theta_f)$  while increases over  $(\theta_f, \mu_+)$ . By the relation shown in Equation (8), we figure out that, for any  $\epsilon \in \left[0, \frac{\mu_+ - \mu_-}{2}\right]$  and  $K \in (1, B_K]$ ,

$$\mathbb{E} \left[ \Delta \left( X, f_{\theta_f(\epsilon)} \right) \right] \geq \mathbb{E} [\Delta(X, f_{\theta_f})] \geq \mathbb{E} [\Delta(X, f_{\theta_f})].$$

Moreover,  $\theta_f$  is the minimizer of the average distance  $\mathbb{E}[\Delta(X, f_\theta)]$  over the interval  $[\mu_-, \mu_+]$ .  $\square$

#### Proof of Theorem 6.5

*Proof.* First off, notice that  $\theta_f(\lambda)$  is the minimizer of  $\mathcal{L}_\theta^{\text{nat}} + \lambda \cdot \mathcal{L}_\theta^{\text{fair}}$  over  $[\mu_-, \mu_+]$ , where  $\mathcal{L}_\theta^{\text{fair}}$  is a shorthand for

$$|\Pr(f_\theta(X) \neq 1 \mid Y = 1) - \Pr(f_\theta(X) \neq -1 \mid Y = -1)|.$$

Thus,  $\mathcal{L}_\theta^{\text{nat}} + \lambda \cdot \mathcal{L}_\theta^{\text{fair}}$  can be presented in a piecewise way as follows:

1) if  $\theta \leq \theta_f$ ,

$$\begin{aligned} \mathcal{L}_\theta^{\text{nat}} + \lambda \cdot \mathcal{L}_\theta^{\text{fair}} &= (1 - \lambda) \Pr(f_\theta(X) \neq 1 \mid Y = 1) + \\ &\quad (1 + \lambda) \Pr(f_\theta(X) \neq -1 \mid Y = -1); \end{aligned}$$

2) if  $\theta > \theta_f$ ,

$$\begin{aligned} \mathcal{L}_\theta^{\text{nat}} + \lambda \cdot \mathcal{L}_\theta^{\text{fair}} &= (1 + \lambda) \Pr(f_\theta(X) \neq 1 \mid Y = 1) + \\ &\quad (1 - \lambda) \Pr(f_\theta(X) \neq -1 \mid Y = -1). \end{aligned}$$

We start with the first case where  $\theta$  is no greater than  $\theta_f$ . The partial derivative of  $\mathcal{L}_\theta^{\text{nat}} + \lambda \cdot \mathcal{L}_\theta^{\text{fair}}$  is then given by

$$\begin{aligned} \frac{\partial (\mathcal{L}_\theta^{\text{nat}} + \lambda \cdot \mathcal{L}_\theta^{\text{fair}})}{\partial \theta} &= \frac{1 - \lambda}{2\sqrt{2\pi}K} \exp\left(-\frac{(\theta - \mu_+)^2}{2K^2}\right) - \\ &\quad \frac{1 + \lambda}{2\sqrt{2\pi}} \exp\left(-\frac{(\theta - \mu_-)^2}{2}\right). \quad (24) \end{aligned}$$

Observe that, when  $\lambda \in [0, 1]$ , this partial derivative is increasing over  $[\mu_-, \theta_f]$  with its value at  $\theta_f$  no greater than 0 while it is always non-positive for any  $\lambda \in (1, +\infty)$  and  $\theta \in [\mu_-, \theta_f]$ . Therefore, the partial derivative presented in Equation (24) proves to be non-positive, whatever  $\lambda$ , which implies that the function  $\mathcal{L}_\theta^{\text{nat}} + \lambda \cdot \mathcal{L}_\theta^{\text{fair}}$  decreases over  $[\theta, \theta_f]$  and we merely need to focus on the case of  $\theta \in [\theta_f, \mu_+]$  in pursuit of its minimizer. Then, we continue to investigate the case where  $\theta$  is greater than  $\theta_f$ . Likewise, the partial derivative of  $\mathcal{L}_\theta^{\text{nat}} + \lambda \cdot \mathcal{L}_\theta^{\text{fair}}$  can be expressed as

$$\begin{aligned} \frac{\partial (\mathcal{L}_\theta^{\text{nat}} + \lambda \cdot \mathcal{L}_\theta^{\text{fair}})}{\partial \theta} &= \frac{1 + \lambda}{2\sqrt{2\pi}K} \exp\left(-\frac{(\theta - \mu_+)^2}{2K^2}\right) - \\ &\quad \frac{1 - \lambda}{2\sqrt{2\pi}} \exp\left(-\frac{(\theta - \mu_-)^2}{2}\right). \quad (25) \end{aligned}$$

We split our studies into the following three scenarios:

- 1) if  $\lambda \in \left[0, \frac{K-1}{K+1}\right]$ ,  $\mathcal{L}_\theta^{\text{nat}} + \lambda \cdot \mathcal{L}_\theta^{\text{fair}}$  first decreases over  $[\theta_f, \theta_f(\lambda)]$  and then increases over  $[\theta_f(\lambda), \mu_+]$  where its minimum takes place at

$$\mu_- - \frac{\mu_+ - \mu_-}{K^2 - 1} + \frac{K}{K^2 - 1} \sqrt{2(K^2 - 1) \ln \left( \frac{1 - \lambda}{1 + \lambda} \cdot K \right) + (\mu_+ - \mu_-)^2}; \quad (26)$$

- 2) if  $\lambda \in \left(\frac{K-1}{K+1}, 1\right]$ , the partial derivative in Equation (25) turns out to be increasing in  $\theta$  with its value at  $\theta_f$  non-negative. It implies that the partial derivative is always non-negative and, thus, the function  $\mathcal{L}_\theta^{\text{nat}} + \lambda \cdot \mathcal{L}_\theta^{\text{fair}}$  increases over  $[\theta_f, \mu_+]$ . As a consequence, the minimizer  $\theta_f(\lambda)$  actually coincides with  $\theta_f$ .
- 3) if  $\lambda \in (1, +\infty)$ , note that the partial derivative is always positive. Following the same reasoning in the previous scenario, we figure out that the minimizer  $\theta_f(\lambda)$  is identical to  $\theta_f$ .

Since the function  $\lambda \mapsto \frac{1-\lambda}{1+\lambda}$  is decreasing over  $\left[0, \frac{K-1}{K+1}\right]$ , by Equation (26), we can argue that  $\theta_f(\lambda)$  is decreasing in  $\lambda$  over  $\mathbb{R}_+$  as well. Furthermore, by the proof of Theorem 6.4, the average distance to the decision boundary is an increasing function in  $\theta$  over  $[\theta_f, \mu_+]$ , which indicates that the average distance associated with the classifier  $f_{\theta_f(\lambda)}$  decreases, as  $\lambda$  increases.  $\square$

## B. Fairness and Robustness Models

### B.1. Fair models

The main text mainly discussed penalty-based methods as a way to encourage accuracy parity in a classifier. This section discusses a second methodology to achieve fairness denoted *group-loss focused* methods [22]. We will show that the main conclusion of this paper (e.g., that fairness increase adversarial vulnerability) holds regardless of the methodology adopted to achieve fairness.

**Group-loss focused methods.** Methods in this category force the training to focus on the loss component of worst performing groups. An effective method to achieve this goal was proposed in [22]:

$$\theta_f = \operatorname{argmin}_\theta \sum_{a \in \mathcal{A}} \frac{1}{q+1} \mathcal{L}_\theta(D_a)^{q+1}, \quad (27)$$

where  $q$  is a non-negative constant. The intuition behind powering the loss by positive number  $q+1$  is to penalize more the classes that have the larger losses. Thus,  $q$  plays the role of the fairness parameter, like  $\lambda$  in penalty-based methods: larger  $q$  or  $\lambda$  values are associated with fairer (but also

often less accurate) models. The main differences between penalty-based methods and group-loss focused methods are the following. First, the loss function of group-loss focused methods is fully differentiable, in contrast to that of penalty-based methods, which is sub-differentiable when the group loss equals the population loss. Second, penalty-based methods try to equalize the losses across various subgroup, while group-focused based methods attempt at minimizing the maximum loss across all subgroups.

## C. Datasets and Settings

**Datasets.** Experiments were performed using three benchmark datasets: UTK Face [48], CIFAR-10 [20], and Fashion MNIST (FMNIST) [43].

1. UTK Face [48]. It consists of more than 20,000 facial images of 48x48 pixels resolution. The experiments consider two learning tasks: (1) The first splits the data into five ethnicities: White, Black, Asian, Indian, and Others. (2) The second splits the data into nine age bins: under-ten years old, 10-14, 15-19, 20-24, 25-29, 30-39, 40-49, 50-59, and over 59 years old. The classes are not uniformly distributed per number of groups and do not contain the same number of images in each group. An 80/20 train-test split is performed.
2. CIFAR-10 [20]. It consists of 60,000 32x32 coloured images belonging to 10 classes, with 6000 images per class. The training set has 50,000 images while the test set has 10,000 images.
3. Fashion MNIST(FMNIST) [43]. It consists of 60,000 28x28 gray-colored images belonging to 10 classes, with 6000 images per class. The training set has 50,000 images while the test set has 10,000 images.

**Network architectures.** The experiments consider three network architectures of increasing complexity:

1. A CNN consisting of 3 convolutions layers followed by 3 fully connected layers.
2. A ResNet 50 network [13] (over 23 million parameters).
3. A VGG-13 network [32] (138 million parameters).

We use CNN to provide some examples in the main text, but in this Appendix we will focus on the ResNet and VGG networks.

**Fair models and parameter settings.** For penalty-based methods the experiments vary the range of fairness parameter  $\lambda \in [0, 2]$ . We note that larger  $\lambda$  values may have a detrimental effects to the models accuracy, which, we believe, limit

the applicability of the fairness methods in real use cases, thus we focus on these more realistic scenarios. However, we also note that appropriate choices of hyperparameters  $\lambda$  will necessarily depend on the task and architecture at hand and can be used to balance the trade-off between accuracy and fairness.

For group-loss focused methods, the experiments consider  $q \in [0, 2]$  for similar reasons as those stated above.

The set of hyper-parameters, learning rate (lr), batch-size (bs), and number of training epochs (epochs) adopted, for each dataset and architecture is reported in Table 1.

| Dataset  | lr   | bs | epochs |
|----------|------|----|--------|
| UTK Face | 1e-3 | 32 | 70     |
| CIFAR-10 | 1e-2 | 32 | 200    |
| FMNIST   | 1e-2 | 32 | 50     |

Table 1. Hyperparameters settings for each dataset.

For each setting, the experiments report the average results of 10 runs, each initializing the models parameters using a different random seed.

**Adversarial attacks.** The experiments also consider two classes of adversarial attacks to test the model robustness: (1) The  $l_\infty$  RFGSM attacks [37] and (2) The  $l_2$  PGD attacks [24]. The experiments adopt the implementations reported in the Python package *torchattacks* [18].

**Code and Preprocessing.** Follow standard setting, the range of the pixel values was normalized in  $[0, 1]$  for all datasets adopted.

All codes were written in Python 3.7 and in Pytorch 1.5.0. The library *torchattacks* [18] was adopted to generate different adversarial attacks. The repository contained the dataset and implementation will be released publicly upon paper acceptance.

## D. Additional experiments

This section describes additional experiments to further support the claims reported in the main paper. In particular, the experiments report results for deeper networks (e.g., ResNet-50) and for additional fairness methods and adversarial attacks.

### D.1. Fairness impacts on the decision boundary

Recall, from Theorem 6.5, that fairness reduces the average distance of the testing samples to the decision boundary. As a consequence the fair classifiers are more vulnerable against the adversarial attacks than the natural (unfair) classifiers. This section provides additional evidence to support

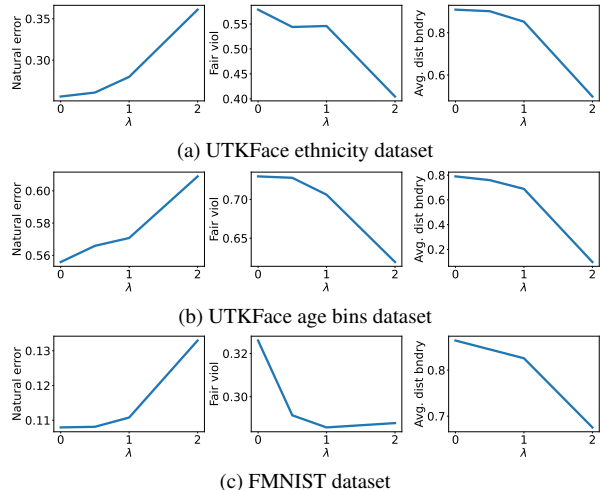


Figure 9. Natural errors (left), fairness violations (middle), and average distance to the decision boundary (right) for different datasets when varying the fairness parameter  $\lambda$  of **penalty-based methods** on ResNet-50 networks

this claim on a high-dimensional model (ResNet 50) and using both penalty based methods additional and group-loss focused methods (see Section B.1) to derive a fair classifier.

**Penalty-based methods.** Figure 9 and Figure 10 summarize the results obtained by a penalty-based fair model executed on different benchmark datasets. The experiments again report a consistent trend: as more fairness is enforced (increasing the values  $\lambda$ ), the natural errors (left plots) generally increase while both the fairness violations (middle plots) and the average distance to the decision boundary (right plots) decrease. Recall that the latter is a proxy for measuring the model robustness: the closer are samples to the decision boundary the less robust is a model. Thus the previous plots show that robustness decreases as fairness increase.

**Group-loss focused methods** A similar setting is reported for a model satisfying fairness using the group-loss focused method described in section B.1. This method maximizes the worst group accuracy, which, in turn, attempts at equalizing the accuracy across groups. Figure 11 reports the results obtained using VGG-13 and the UTK-Face dataset. The results again illustrate similar trends: as the fairness parameter  $q$  increases, the natural errors (right) tend to increase while both the fairness violations (middle) and the average distance to the decision boundary (left) decrease. Notice that small enough  $q$ -values may also act as a regularizer and have a beneficial effect toward the natural error, as observed for the UTK-age bin task (bottom-left plot).



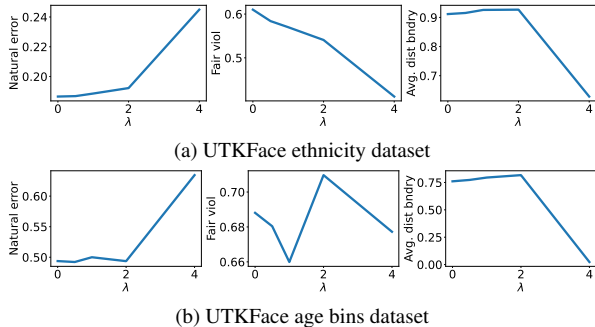


Figure 10. Natural errors (left), fairness violations (middle), and average distance to the decision boundary (right) for different datasets when varying the fairness parameter  $\lambda$  of **penalty-based methods** on VGG 13 networks

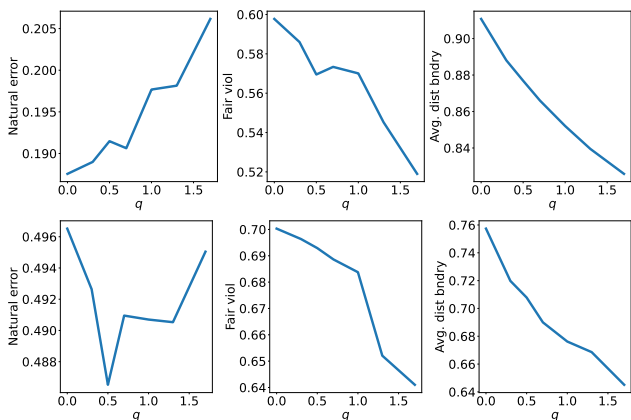


Figure 11. Natural errors, fairness violations, and average distance to the decision boundary for the UTK-Face *ethnicity* (top), UTK-Face *age bins* (bottom) datasets when varying the fairness parameter  $q$  of **group-loss focused methods** on VGG-13 networks.

## D.2. Boundary errors increase as fairness decreases

This section provides additional experiments to illustrating that the result of the paper (*fairness increases the adversarial vulnerability*) is invariant across different fair classifier implementations. The experiments adopt the group-loss focused methods for different values of the fairness parameter  $q$ . Notice that a natural classifier is obtained when  $q = 0$ . Figure 12 displays the natural (left) and boundary (center) errors attained under different level of RFGSM attacks (regulated by parameter  $\epsilon$ ) and the fairness violation (right) on CIFAR (top) FMNIST (middle) and UTK (bottom) datasets. Notice how increasing  $q$  to large enough values typically decreases the fairness violations. However, this comes at the cost of increasing the natural error and the boundary errors, which, in turn, exacerbate the robust errors.

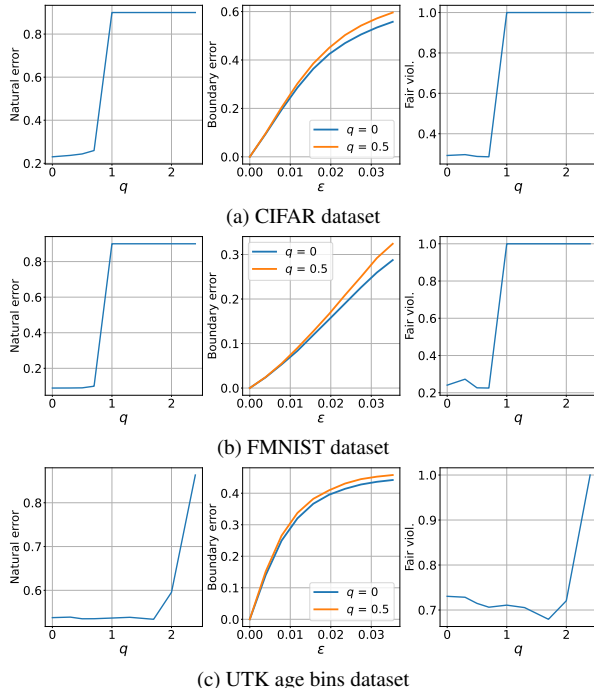


Figure 12. Natural errors (left), boundary error under different RFGSM attacks (middle), and fairness violation (right) of **group-focused methods** on ResNet-50 networks

## D.3. A Mitigating Solution with Bounded Losses

**More intuition why bounded loss works.** This section first provides more intuition about why bounded loss functions, such as the ramp loss adopted in the main text, can help reducing the impacts of fairness towards robustness. To guide the intuitions, we will refer to Figure 13, which plots the graph functions of the following loss function for binary classification tasks:

- Ramp loss [7, 10], defined by:

$$\ell(f_{\theta}(X), Y) = \min(1, \max(0, 1 - Y f_{\theta}(X))).$$

- Log-loss [12], defined by:

$$\ell(f_{\theta}(X), Y) = \log(1 + \exp(-Y f_{\theta}(X))).$$

- Exponential loss [12], defined by:

$$\ell(f_{\theta}(X), Y) = \exp(-Y f_{\theta}(X)).$$

Notice that, as illustrated in Figure 13, unbounded losses (such as log-loss or exponential loss) amplify the classification errors of misclassified samples  $X$ , in a way proportionately to the distance of  $X$  from the decision boundary. The misclassification of a sample is captured by the expression  $f_{\theta}(X)Y < 0$ , while the distance to the decision boundary

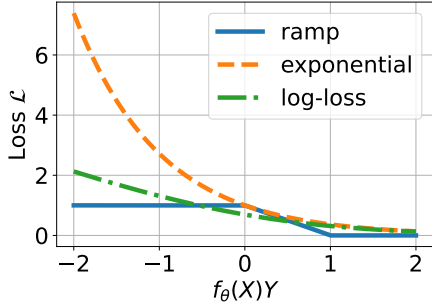


Figure 13. Illustration of different loss functions

by expression  $|f_\theta(X)Y|$  (x-axis). Notably these losses are unbounded.

Now notice that a consequence of training a fair classifier is to push its decision boundary to dense region of the advantaged group. This is because such classifier attempts at aligning the groups classification losses, i.e.,  $\mathbb{E}[\ell(f_\theta(X), Y)|Y = -1] = \mathbb{E}[\ell(f_\theta(X), Y)|Y = 1]$ . When the decision boundary is moved closer to the input samples, the classifier will inevitably become less robust to small perturbations of adversarial noise.

On the contrary, using a bounded loss function, such as ramp loss, during fair learning, can greatly reduce the impact produced by such (outlier) samples.

**Effectiveness of the mitigation solution.** Next, this section provides additional experiments to demonstrate the effectiveness of the proposed solution to find a good trade-off between fairness and robustness. The generality of the proposed solution is demonstrated across several architectures (VGG-13 and ResNet 50) and adversarial attacks ( $\ell_\infty$  RFGSM and  $\ell_2$  PGD attacks under different level of attacks  $\epsilon$ ).

In summary, the proposed mitigation solution—which uses a bounded loss—result in classifiers that, in the vast majority of the cases, are fairer and more robust than those produced by models using a standard (cross entropy) loss.

**VGG-13 and  $\ell_\infty$  RFGSM attacks.** Figures 14 and 15 report the boundary errors attained using RFGSM attacks on fair ( $\lambda > 0$ ) and regular ( $\lambda = 0$ ) classifiers on CIFAR and UTK datasets, respectively and using a VGG 13. The plots compare models obtained using a cross entropy loss (top plots) and those using a Ramp loss (bottom plots).

**VGG-13 and  $\ell_2$  PGD attacks.** Figures 16 and 17. report the boundary errors attained using a PGD attacks on fair ( $\lambda > 0$ ) and regular ( $\lambda = 0$ ) classifiers on UTK datasets and using a VGG 13. Once again, the plots compare models

obtained using a cross entropy loss (top plots) and those using a Ramp loss (bottom plots).

**ResNet 50 and  $\ell_\infty$  RFGSM attacks** Figures 18 and 19. report the boundary errors attained using a RFGSM attacks on fair ( $\lambda > 0$ ) and regular ( $\lambda = 0$ ) classifiers on UTK Face and FMNIST datasets, respectively and using a ResNet50. Once again, the plots compare models obtained using a cross entropy loss (top plots) and those using a Ramp loss (bottom plots).

**ResNet 50 and  $\ell_2$  PGD attacks** Figures 20 and 21 report the boundary errors attained using a PGD attack on fair ( $\lambda > 0$ ) and regular ( $\lambda = 0$ ) classifiers on CIFAR10 and FMNIST datasets, respectively, and using a ResNet50. Once again, the plots compare models obtained using a cross entropy loss (top plots) and those using a Ramp loss (bottom plots).

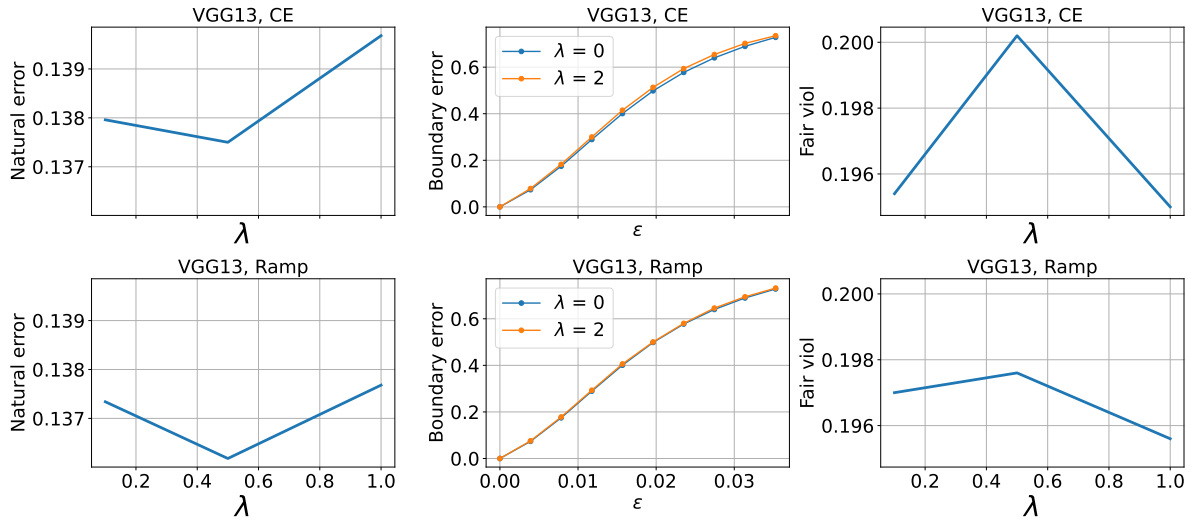


Figure 14. **Top:** Natural errors (left) and fairness violations (right) on the CIFAR-10 *ethnicity* task at varying of the fairness parameters  $\lambda$ . The middle plots compares the robustness of fair ( $\lambda > 0$ ) vs. natural ( $\lambda = 0$ ) classifiers to different RFGSM attack levels. **Bottom:** Mitigating solution using the bounded Ramp loss. The base classifiers are VGG-13.

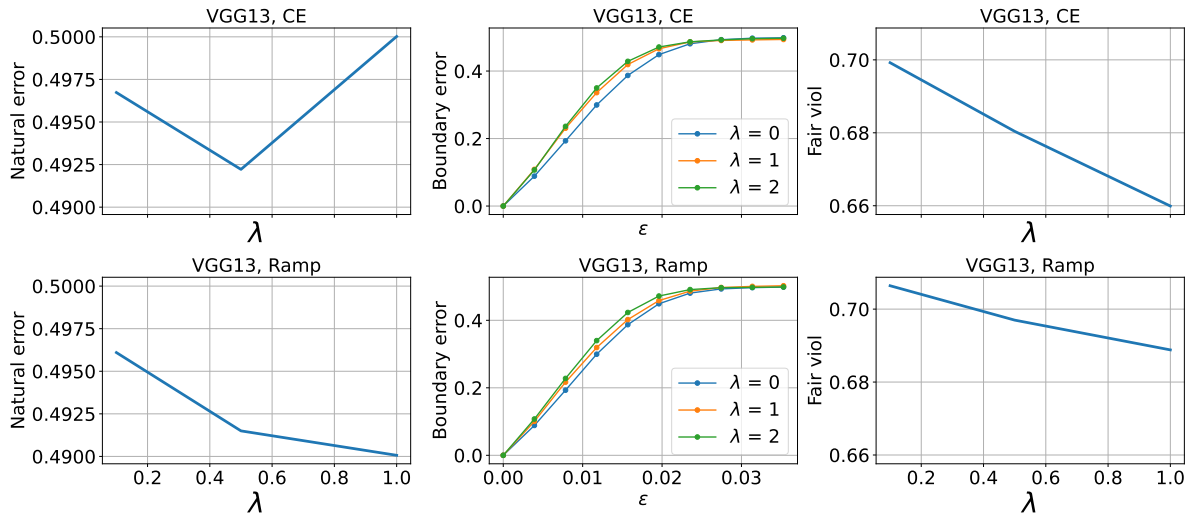


Figure 15. **Top:** Natural errors (left) and fairness violations (right) on the UTKFace *age bins* task at varying of the fairness parameters  $\lambda$ . The middle plots compares the robustness of fair ( $\lambda > 0$ ) vs. natural ( $\lambda = 0$ ) classifiers to different RFGSM attack levels. **Bottom:** Mitigating solution using the bounded Ramp loss. The base classifiers are VGG-13.

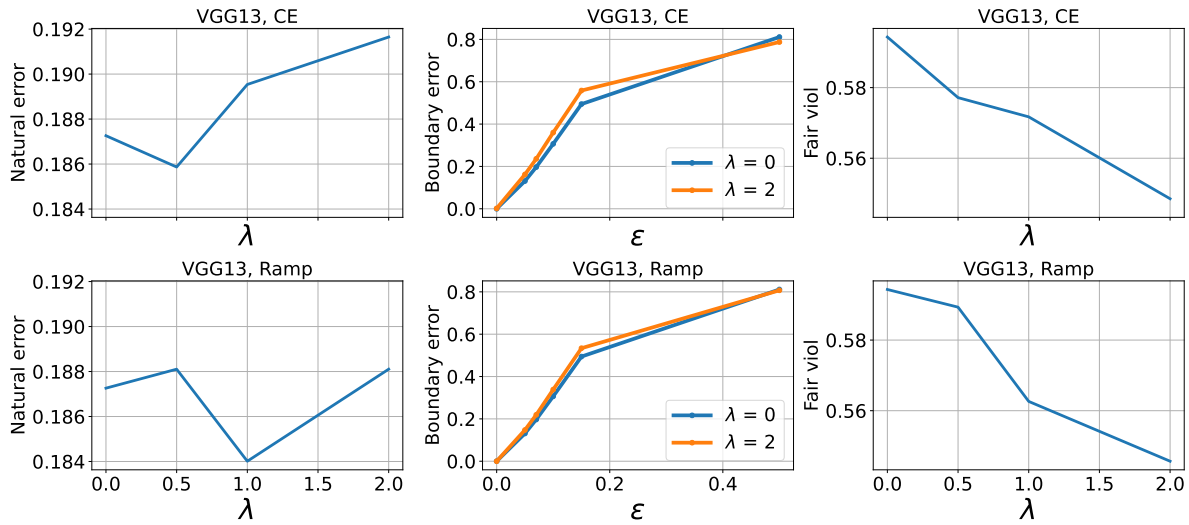


Figure 16. **Top:** Natural errors (left) and fairness violations (right) on the UTKFace *ethnicity* task at varying of the fairness parameters  $\lambda$ . The middle plots compares the robustness of fair ( $\lambda > 0$ ) vs. natural ( $\lambda = 0$ ) classifiers to different  $l_2$  PGD attack levels. **Bottom:** Mitigating solution using the bounded Ramp loss. The base classifier are VGG-13.

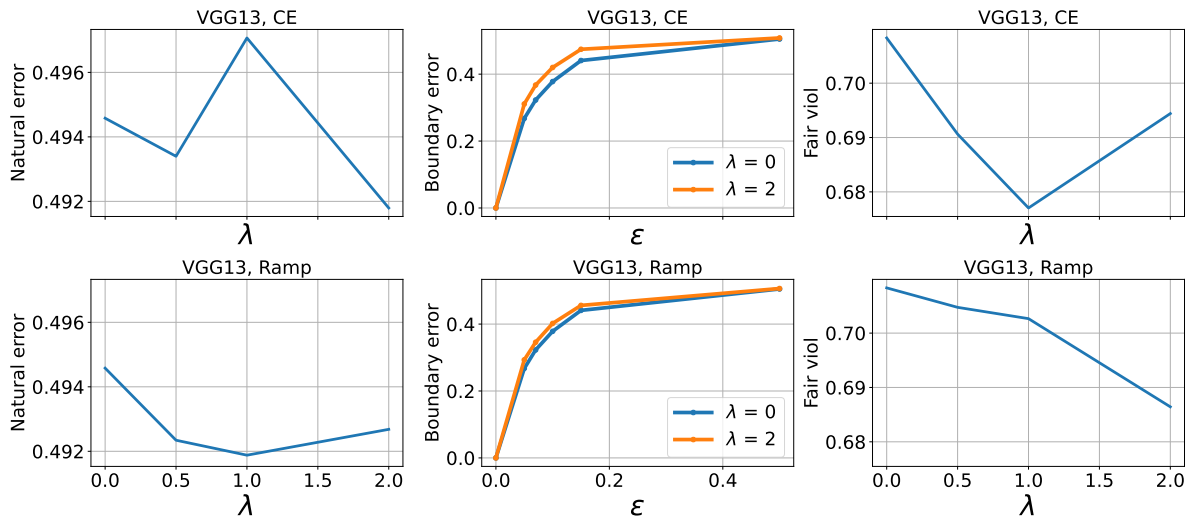


Figure 17. **Top:** Natural errors (left) and fairness violations (right) on the UTKFace *age bins* task at varying of the fairness parameters  $\lambda$ . The middle plots compares the robustness of fair ( $\lambda > 0$ ) vs. natural ( $\lambda = 0$ ) classifiers to different  $l_2$  PGD attack levels. **Bottom:** Mitigating solution using the bounded Ramp loss. The base classifier are VGG-13.



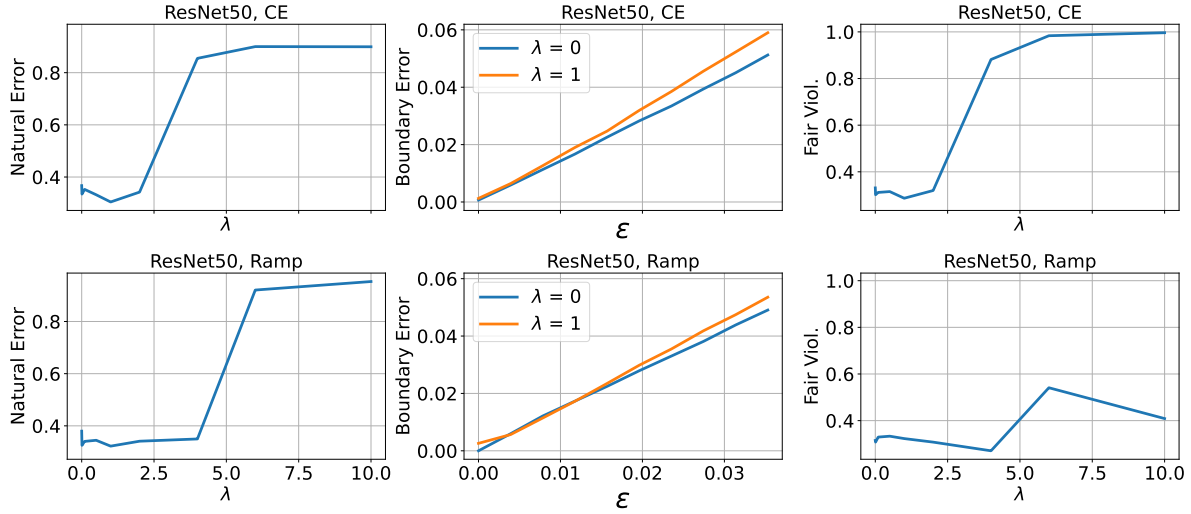


Figure 18. **Top:** Natural errors (left) and fairness violations (right) on the UTKFace *ethnicity* task at varying of the fairness parameters  $\lambda$ . The middle plots compares the robustness of fair ( $\lambda > 0$ ) vs. natural ( $\lambda = 0$ ) classifiers to different  $l_\infty$  RFGSM attack levels. **Bottom:** Mitigating solution using the bounded Ramp loss. The base classifier are Res Net 50.

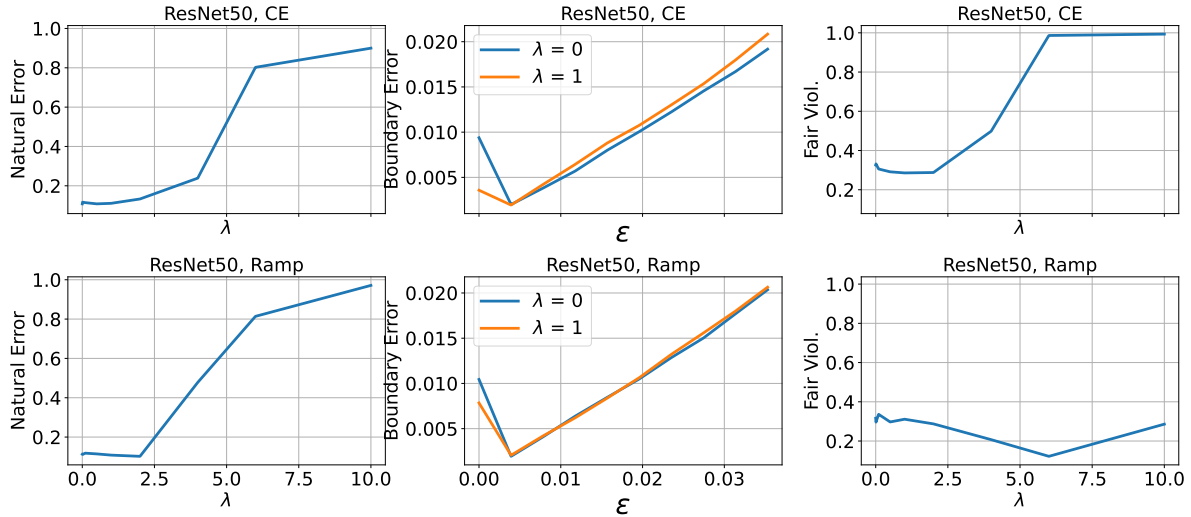


Figure 19. **Top:** Natural errors (left) and fairness violations (right) on the FMNIST task at varying of the fairness parameters  $\lambda$ . The middle plots compares the robustness of fair ( $\lambda > 0$ ) vs. natural ( $\lambda = 0$ ) classifiers to different  $l_\infty$  RFGSM attack levels. **Bottom:** Mitigating solution using the bounded Ramp loss. The base classifier are Res Net 50.

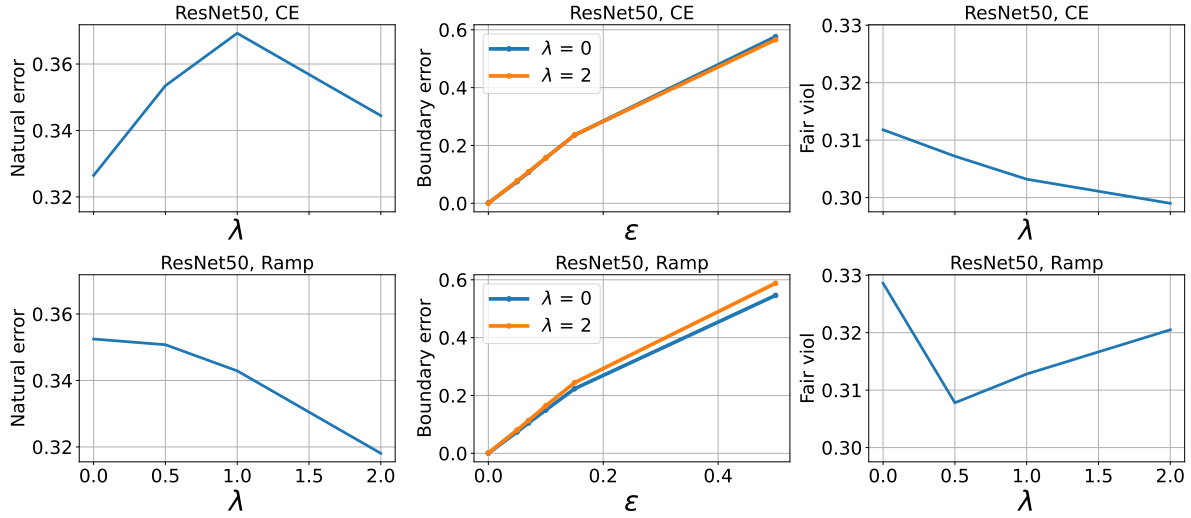


Figure 20. **Top**: Natural errors (left) and fairness violations (right) on the CIFAR 10 task at varying of the fairness parameters  $\lambda$ . The middle plots compares the robustness of fair ( $\lambda > 0$ ) vs. natural ( $\lambda = 0$ ) classifiers to different  $l_2$  PGD attack levels. **Bottom**: Mitigating solution using the bounded Ramp loss. The base classifiers are ResNet 50.

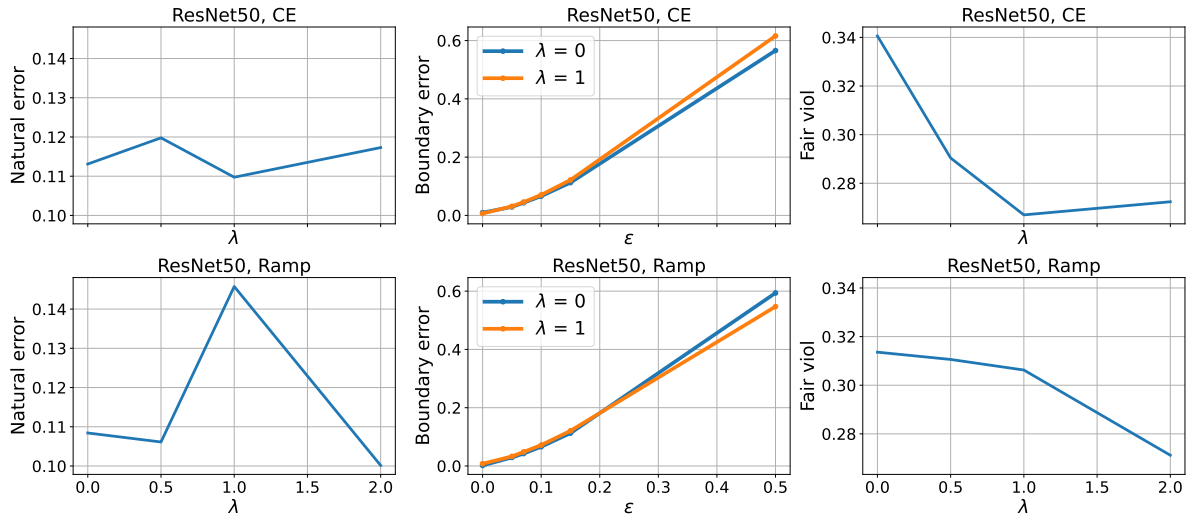


Figure 21. **Top**: Natural errors (left) and fairness violations (right) on the FMNIST task at varying of the fairness parameters  $\lambda$ . The middle plots compares the robustness of fair ( $\lambda > 0$ ) vs. natural ( $\lambda = 0$ ) classifiers to different  $l_2$  PGD attack levels. **Bottom**: Mitigating solution using the bounded Ramp loss. The base classifiers are ResNet 50.